Reply to editorial decision letter and reviewer comments

Dear Editor, dear Keely,

we are very grateful for your great editorial support and your positive editorial decision. Readily we follow your kind invitation to submit a revised version of our manuscript. As recommended by the reviewers, whom we once again cordially thank for their constructive feedback and suggestions, and you, we particularly tried to shorten the MS (reduction from almost 18,000 to less than 13,500 words). We furthermore included clarifications where necessary. Please find a point-by-point reply to your editorial decision letter below.

With best wishes,
Johannes Hepp & Michael Zech (on the behalf of all co-authors)

Reviewer #1: please address all comments included here.

→ We fully agree with Referee #1 that temperature is known to have a strong effect on $\delta^2H/\delta^{18}O_{precipitation}$ (and thus as well on $\delta^2H_{n\text{-alkane}}/\delta^{18}O_{sugar}$). Unlike originally planned (see our reply to Referee #1), we however prefer not to include the reconstructed $\delta^2H/\delta^{18}O_{source\text{-}water}$ record for the Gemündener Maar. Rather, in order not to extend our MS, we simply included the temperature effect now already in the abstract as well as in the revised Fig. 5. Please let us know in case you do not agree with this suggestion.

→ Following the recommendation of Referee #1 we explain 'LEL' earlier in the revised MS and shortened the MS (from almost 18,000 to less than 13,500 words).

SC1: Clarification of the chronology should be included in the revision, however, if this will only add length to the manuscript, I would encourage you to submit a supplementary file that clearly articulates (and graphically represents?) how your chronology was derived. The point regarding coring location is easily clarified in your sites/methods. With regards to cut off for auto/alloch inputs for C/N values, I too would agree with the use of 10.

→ We completely revised the age-depth model as suggested by B. Zolitschka in SC1 and written in our reply. However, we realized this without adding length to the manuscript. We divided the former chapter '2.2 Bulk analysis and age control' into '2.2 Bulk analysis and pollen analysis' and '2.3 Age control'. We also added one figure (new Fig. 2, in combination with new Fig. 3) to the manuscript in order to better illustrate how the age-depth model is derived. Therefore, we did not add a supplementary data file to explain the age-depth model. The coring location and some explanation about the location we added in chapter 2.1.

→ Readily we refer to the C/N threshold of 10 according to Meyers (2003) in our revised MS.

Reviewer #2: Again, mostly relates to reducing bulk, being more succinct and clear throughout.

→ We are very grateful to P.A. Meyers (Referee #2) for his constructive and encouraging comments. Following his recommendation, we shortened and partly rewrote our MS in order to make it more succinct and clear.

SC2: Please include reference in your revision to d-excess, adding in some of the material cited in response (if not already in paper)

→ Readily included in the first paragraph of chapter 3.3

SC3: Again, adding in some of the material included here in a more succinct format would be useful. I realise this reviewer is the least supportive of the work, but some of the other comments you need to address may go some way to reconciling this review. Of course, this review will continue to be available for transparency.

→ We are very grateful for your careful and balanced assessment of SC3. Indeed, Kahmen et al. (2013), where E. Schefuß is co-author, is already cited and discussed thoroughly in terms of dicotyledonous versus monocotyledonous in chapter 3.2.

SC4: Regarding your statement of encouraging the modelling community to use this work in the absence of palaeoclimate modelling as part of this paper - please can you make your data open access and include a link to it (if you have not already done so). I am unsure why you would remove the statistics you have when asked for more? Are there additional analyses that could be undertaken to address the issues raised? If not, rather than remove, please clarify and comment in the manuscript. In the absence of additional analyses, please just ensure that your text does not suggest that correlation = causation, rather be explicit about the similarities and the fact this in itself lends to further investigation and (may) be helped by use of palaeoclimate modelling scenarios.

→ Readily we follow your recommendation and include our data in a supplementary excel file in order to make it available for the modelling community.

→ We prefer to remove the Monte Carlo simulation. In our opinion, further statistical tests and analyses are not essential for the take home message of our MS. We readily follow your recommendation and carefully revised our MS in order to avoid a false correlation = causation interpretation.

References

Meyers, P. A.: Applications of organic geochemistry to paleolimnological reconstructions: a summary of examples from the Laurentian Great Lakes, Organic Geochemistry, 34, 261–289, 2003.

How dry was the Younger Dryas? Evidence from a coupled δ^2H-$\delta^{18}O$ biomarker paleohygrometer~~,~~ applied to the Lake Gemündener Maar sediments, Western Eifel, Germany

Johannes Hepp[a,b,#,1], Lorenz Wüthrich[c], Tobias Bromm[b], Marcel Bliedtner[c,2], Imke Kathrin Schäfer[c], Bruno Glaser[b], Kazimierz Rozanski[d], Frank Sirocko[e], Roland Zech[c,2], Michael Zech[b,f,3]

[a]*Chair of Geomorphology and BayCEER, University of Bayreuth, Universitätsstrasse 30, D-95440 Bayreuth, Germany*

[b]*Institute of Agronomy and Nutritional Sciences, Soil Biogeochemistry, Martin-Luther-University Halle-Wittenberg, Von-Seckendorff-Platz 3, D-06120 Halle, Germany*

[c]*Institute of Geography and Oeschger Center for Climate Change Research, University of Bern, Hallerstrasse 12, CH-3012 Bern, Switzerland*

[d]*Faculty of Physics and Applied Computer Science, AGH University of Science and Technology, Al. Mickiewicza 30, 30-059 Kraków, Poland*

[e]*Institute of Geosciences, Group of Climate and Sediments, Johannes Gutenberg University of Mainz, J.-J.-Becher-Weg 21, D-55128 Mainz, Germany*

[f]*Institute of Geography, ~~Chair of Landscape and Geoecology,~~ Dresden University of Technology, Helmholtzstrasse 10, D-01062 Dresden, Germany*

[#] *corresponding author: johannes-hepp@gmx.de*

[1]Present Address: *Chair of Geomorphology and BayCEER, University of Bayreuth, Universitätsstrasse 30, D-95440 Bayreuth, Germany*

[2]Present Address: *Institute of Geography, Chair of Physical Geography, Friedrich-Schiller University of Jena, Löbdergraben 32, D-07743 Jena, Germany*

[3]Present Address: *Institute of Geography~~, Chair of Landscape and Geoecology~~, Dresden University of Technology, Helmholtzstrasse 10, D-01062 Dresden, Germany*

Abstract

The Late Glacial to Early Holocene transition phase and particularly the Younger Dryas period, i.e. the major last cold spell in Central Europe during the Late Glacial, are considered crucial for understanding rapid natural climate change in the past. The sediments from Maar lakes in the Eifel, Germany, have turned out to be valuable archives for recording such paleoenvironmental changes.

For this study, we investigated a Late Glacial to Early Holocene sediment core that was retrieved from ~~Lake~~ the Gemündener Maar in the Western Eifel, Germany. We analysed the hydrogen (δ^2H) and oxygen ($\delta^{18}O$) stable isotope composition of leaf wax-derived lipid biomarkers (*n*-alkanes C_{27} and C_{29}) and a hemicellulose-derived sugar biomarker~~s~~ (arabinose), respectively. Both $\delta^2H_{n\text{-alkane}}$ and $\delta^{18}O_{sugar}$ are suggested to reflect mainly leaf water of vegetation growing in the catchment of the Gemündener Maar. Leaf water reflects δ^2H and $\delta^{18}O$ of precipitation (primarily temperature-dependent) modified by evapotranspirative enrichment of leaf water due to transpiration. ~~This enables the coupling of the results via a δ^2H-$\delta^{18}O$ biomarker paleohygrometer approach and allows calculating past relative air humidity values, which is the major advantage of the applied approach. Fundamental was the finding that the reconstructed isotopic~~Based on the notion that the ~~enrichment of leaf water due to evapotranspiration, and thus the calculated deuterium-excess of leaf water, depends mainly on ancient~~evapotranspirative enrichment depends primarily on relative humidity (RH), ~~changes. We hence use the~~ we apply a previously introduced 'coupled $\delta^2H_{n\text{-alkane}}$-$\delta^{18}O_{sugar}$ ~~δ^2H-$\delta^{18}O$ biomarker~~ paleohygrometer approach' to reconstruct the deuterium-excess of leaf water and in turn ~~relative air humidity values corresponding to the daytime and vegetation period (~~Late Glacial-Early Holocene RH_{dv}~~)~~ changes from our Gemündener Maar record.

~~Most importantly, the~~Our results do not provide evidence for overall markedly dry climatic conditions having prevailed during the Younger Dryas. ~~of the coupled δ^2H-$\delta^{18}O$ biomarker paleohygrometer approach (i) support~~Rather, a two-phasing of the Younger Dryas is supported with~~, i.e. a relative~~ moderate wet conditions ~~phase (~~on Allerød level~~)~~ during the first half ~~followed by a~~and drier conditions during the second half of the Younger Dryas~~. ending, (ii) do not corroborate overall drier climatic conditions characterising the Younger Dryas or a two-phasing with regard to a first dry and cold Younger Dryas phase followed by a warmer period along with increasing precipitation amounts, and (iii)~~ Moreover, our results suggest that the amplitude of RH_{dv} changes during the Early Holocene was more pronounced ~~compared to~~than during the Younger Dryas. This included the occurrence of a 'Preboreal Humid Phase'. One possible ~~driver~~ explanation for ~~the~~ this unexpected ~~Lake Gemündener Maar~~

~~RH_{dv} variations~~finding could be that~~the~~ solar activity is a hitherto underestimated driver of Central European RH changes in the past.

1 Introduction

In order to evaluate the relevance of man-made climate change in the future, it is of great importance to study and understand large and rapid climate fluctuations in the past. Many studies have focused on the Late Glacial to Early Holocene transition phase, a period with various expressions in temperature, atmospheric circulation and hydrology worldwide (Alley, 2000; Brauer et al., 2008; Denton et al., 2010; Partin et al., 2015; Wagner et al., 1999). Particularly the Younger Dryas (YD) period, i.e. the major last cold spell in Central Europe during the Late Glacial just before the onset of the Holocene warm period (Denton et al., 2010; Heiri et al., 2014; Isarin and Bohncke, 1999), has long been considered crucial for understanding rapid natural climate change in the past (Alley, 2000). The sediments from maar lakes in the Eifel, Germany, have turned out to be valuable archives for paleoenvironmental reconstructions providing high resolution palynological, sedimentological and geochemical records for climate, vegetation and landscape history (Brauer et al., 2008; Brunck et al., 2015; Litt et al., 2003; Litt and Stebich, 1999; Sirocko et al., 2013; Zolitschka, 1998).

Lacustrine sedimentary lipid biomarkers such as *n*-alkanes, originating either from leaf waxes of higher terrestrial plants (Eglinton and Hamilton, 1967) or from aquatic organisms (Volkman et al., 1998), and especially their hydrogen isotope composition ($\delta^2H_{n\text{leaf-wwax/}n\text{-alkane}}$), are widely accepted as paleoclimate proxies (Huang et al., 2004; Mügler et al., 2008; Sachse et al., 2004, 2012; Sauer et al., 2001). It has been demonstrated that $\delta^2H_{\text{leaf-wax/}n\text{-alkane}}$ the hydrogen isotope composition of the leaf waxes is well correlated with hydrogen isotope composition of precipitation (δ^2H_{prec}) (e.g. Hou et al., 2008; Rao et al., 2009). This confirms the great potential to establish records of the stable isotope composition of past precipitation (Sachse et al., 2012), s Similar to the well-known ice-core and speleothem records from Greenland and from speleothems (Alley, 2000; Luetscher et al., 2015; Rasmussen et al., 2014), lacustrine $\delta^2H_{\text{leaf-wax/}n\text{-alkane}}$ records are therefore increasingly used to reconstruct δ^2H of past precipitation and thus for deriving paleoclimatic information which among others provide information about changes of surface air temperature in the past (c.f. Araguás-Araguás et al., 2000; Dansgaard, 1964; Rozanski et al., 1993). However, the alteration of δ^2H_{prec} precipitation stable isotope signal either through evapo(transpi)rative ^2H enrichment of leaf or lake water enrichment can challenge a direct robust δ^2H_{prec} reconstruction of δ^2H_{prec} based on $\delta^2H_{n\text{-alkane}}$ alone (Kahmen et al., 2013a; Mügler et al., 2008; Sachse et al., 2012(e.g. Mügler et al., 2008; Zech et al., 2015). Apart from $\delta^2H_{n\text{-alkane}}$, the oxygen isotope composition of hemicellulose/polysaccharide-derived sugars ($\delta^{18}O_{sugar}$) was established as a tool in paleoclimate research during the last years (Zech et al., 2011, 2013a, 2014a). Analogous to

$\delta^2H_{n\text{-alkane}}$, $\delta^{18}O_{sugar}$ is affected by the isotope composition of source water, which is closely related to the local precipitation ($\delta^{18}O_{prec}$), as well as by evapotranspirative ^{18}O enrichment (Tuthorn et al., 2014; Zech et al., 2013b, 2014b). ~~However, the overall challenge of disentangling between the source water signal and changes caused by evapotranspiration can be~~Moreover, it was suggested that the coupling of δ^2H and $\delta^{18}O$ results ~~potentially resolved by using a coupled δ^2H-$\delta^{18}O$ approach~~can help to disentangle between $\delta^2H/\delta^{18}O_{prec}$ changes and variable $^2H/^{18}O_{leaf/lake\text{-}water}$ enrichment (Henderson et al., 2010; Hepp et al., 2015, 2017; Tuthorn et al., 2015; Voelker et al., 2014, 2015; Zech et al., 2013a). ~~While~~ For instance, Voelker et al. (2014) presented a framework for using δ^2H and $\delta^{18}O$ of tree-ring cellulose in order to infer relative air humidity (RH). ~~And,~~ Tuthorn et al. (2015) validated a previously suggested 'coupled $\delta^2H_{n\text{-alkane}}$-$\delta^{18}O_{sugar}$ paleohygrometer approach'. Accordingly, the application of that approach to ~~using leaf wax-derived *n*-alkanes and hemicellulose-derived sugars, showing the potential to reconstruct mean relative air humidity changes along~~ an Argentinian topsoil transect yielded a highly significant correlation of actual and biomarker-based reconstructed RH values ($R = 0.79$, $p < 0{,}001$, $n = 20$). Both approaches were successfully applied to loess-paleosol sequences (Hepp et al., 2017; Zech et al., 2013a) and sub-fossil wood (Voelker et al., 2015). By contrast, ~~whereas~~ the application of the 'coupled $\delta^2H_{n\text{-alkane}}$-$\delta^{18}O_{sugar}$ paleohygrometer approach' to a ~~δ^2H-$\delta^{18}O$ coupling using terrestrial biomarkers in~~ lacustrine archive~~s~~ is still missing. ~~Indeed, already Sternberg (1988) suggested the coupling of aquatic δ^2H of lipids and $\delta^{18}O$ cellulose in order to tangle lake water isotope composition more robustly, due to challenges of using δ^2H values of nitro-cellulose derived from lake sediments. Hence, coupled δ^2H-$\delta^{18}O$ biomarker approaches applied to lacustrine archives were used to decipher between lake water evaporation history and changes in the isotope composition of the lake water input (Henderson et al., 2010; Hepp et al., 2015), based on a combination of δ^2H of palmitic acid and $\delta^{18}O$ of carbonate as well as $\delta^2H_{n\text{-alkane}}$ and $\delta^{18}O_{sugar}$ records. Deriving quantitative relative humidity values is challenging without additional hydrological input parameters, due to past lake mass balance changes (e.g. Wolfe et al., 2001). However, quantitative paleoclimate changes from biomarker-isotope proxy data, like a relative humidity record, may be useful to assess atmospheric circulation pattern changes in the past (Voelker et al., 2015), which was so far challenging due to a lack of applicable quantitative model approaches (Feng et al., 2007; Rach et al., 2014). Terrestrial *n*-alkane and sugar biomarker-based isotope records from Lake Gemündener Maar sediments, which are coupled in a δ^2H-$\delta^{18}O$ paleohygrometer approach, have the potential to fill this gap by deriving a more robust relative air humidity record for Central Europe for the Late Glacial and Early Holocene transition.~~

~~This~~ Within this study we aimed at applying the coupled $\delta^2H_{n\text{-alkane}}$-$\delta^{18}O_{sugar}$ paleohygrometer approach to the Late Glacial-Early Holocene sediment cores of the Gemündener Maar. ~~was conducted based on~~More specifically, we addressed the following objectives: (i) source identification of the sedimentary organic matter and the investigated *n*-alkanes and sugars (aquatic vs. terrestrial), (ii) reconstructing leaf water isotope composition based on compound-specific δ^2H and $\delta^{18}O$ values of the *n*-alkane and sugar biomarkers, (iii) reconstructing ~~relative air humidity~~RH changes ~~via~~ using the coupled $\delta^2H_{n\text{-alkane}}$-$\delta^{18}O_{sugar}$ paleohygrometer approach and (iv) inferring ~~new~~ implications for middle European paleoclimate history from the established ~~Lake~~ Gemündener Maar ~~relative air humidity~~RH record ~~for the Late Glacial and Early Holocene transition. Overall, the potentials and limitations of the coupled $\delta^2H_{n\text{-alkane}}$-$\delta^{18}O_{sugar}$ paleohygrometer approach applied to lacustrine archive will be discussed~~.

2 Material & Methods

2.1 ~~Lake~~ The Gemündener Maar and sampling

~~Lake~~ The Gemündener Maar is located in the Eifel volcanic fields in western Germany at an altitude of 407 m a.s.l. (50°10'39.853"N, 6°50'12.912"E; Fig. 1A and B; Sirocko et al., 2013). The ~~Maar~~ maar was formed during a phreatomagmatic explosion within the local Devonian siltstone (greywacke) around 20-25 ka BP (Büchel, 1993). The lake is 39 m deep at maximum and has a diameter of roughly 300 m. Due to its formation conditions the lake is almost circular with a lake surface area of 75,000 m^2 and is surrounded by a small catchment (Fig. 1B), with an area of 430,000 m^2 (Scharf and Menn, 1992). The lake is fed by precipitation and groundwater (no surface inflow and outflow present). The sediments are, accordingly, not affected by fluvial sediment input. The catchment area is furthermore steep and densely vegetated with broad-leaved trees (Fig. 1C). The investigated samples were taken from the 8 m Gemündener Maar core (GM1), which was taken at approximately 20 m water depth near the center of the maar (Fig. 1B) with a Livingston piston corer (UWITEC, Mondsee, Austria). The GM1 core was retrieved from a terrace on the steep slope of the maar exactly in a fan of an underwater erosion gully structure. The core is part of the Eifel Laminated Sediment Archive Project of the Institute for Geoscience at Johannes Gutenberg University Mainz (Sirocko et al., 2013, 2016).

(Fig. 1)

2.2 Bulk analysis and pollen analysis~~age control~~

Bulk analyses were carried out on 112 samples, covering a section of 606 cm to 727 cm depth of the Gemündener Maar GM1 core. Total carbon (TC~~),~~) and ~~total organic~~ nitrogen (~~TO~~N), bulk carbon isotope composition ($\delta^{13}C_{TC}$) and nitrogen isotope composition ($\delta^{15}N$) were determined at the Institute of Agronomy and Nutritional Sciences, Soil Biogeochemistry, Martin-Luther-University Halle-Wittenberg, using an EuroVector EA 3000 elemental analyzer (Hekatech, Wegberg, Germany) coupled via a Conflo III Interface to a Delta V Advantage isotope ratio mass spectrometer (IRMS; both from Thermo Fisher Scientific, Bremen, Germany). Additionally, total organic carbon (TOC) and bulk $\delta^{13}C$ of the total organic carbon ($\delta^{13}C_{TOC}$) were assessed after removal of carbonate with 32% hydrochloric acid (HCl) fumigation followed by a neutralization step with moist sodium hydroxide~~NaOH~~, both for 24 h under 60°C and vacuum conditions. This allows calculating ~~carbon to nitrogen ratio based on total organic contents (~~TOC/~~TO~~N~~).~~ ratios. Laboratory standards from the International Atomic Energy Agency (IAEA) as well as from United States Geological Survey (USGS) with known total carbon, nitrogen, ^{13}C and ^{15}N contents (IAEA N2, IAEA CH6, IAEA NO3, IAEA CH7, IAEA 305A, USGS 41) were used for calibration. The ^{13}C and ^{15}N contents are expressed in the common δ-notation as relative to an international standard ($\delta^{13}C$: Vienna Pee Dee Belemnite, VPDB; $\delta^{15}N$: atmospheric N_2, Air). ~~It should be noted that TON and ^{15}N contents are only reported for measurements prior to carbonate removal. This is based on Walthert et al. (2010) and Harris et al. (2001), who reported lower N contents and slightly more positive $\delta^{15}N$ after HCl fumigation, respectively. Bulk analyses were carried out on 112 samples, covering a section of 606 cm to 727 cm depth of the Lake Gemündener Maar GM1 core.~~

For pollen analysis, 16 samples were investigated covering the relevant depth section. Each sample~~s contained~~covered a depth range of 1 cm. Preparation was conducted by F. Dreher according to standard procedures at the laboratory of the Group of Climate and Sediments, Institute of Geosciences, Johannes Gutenberg University of Mainz, using potassium hydroxide, HCl and hydrofluoric acid (Sirocko et al., 2016). Afterwards, acetic acid and a mixture of acetic anhydride and sulphuric acid (9:1) were used for acetolysis. The samples were then centrifuged at 3000 to 3500 rounds per minute for 5 min and then sieved over 200 µm and a 10 µm sieve. Afterwards, the samples were fixed with anhydrous glycerol for reliable identification and a maximum magnification of 600 was used for counting the remains. Pollen results ~~were~~are reported in relative percentages (%).

2.3 Age control

The investigated sediments are partially laminated. The ~~second~~first tie point to establish a chronology for the ~~Lake~~ Gemündener Maar core is a radiocarbon-dated piece of charcoal in 727 cm core depth, which dated to 13,800 ± 110 cal a BP (Fig. 2~~C~~D). This age is derived from a ^{14}C age of 11,950 ± 65 a BP as part of the supplement material of Sirocko et al. (2013), calibrated using CalPal-software (Weninger and Jöris, 2008) calculated with the IntCal13 calibration curve (Reimer et al., 2013). The uncertainty of the calibrated ^{14}C age represents the 68% probability range. ~~and~~ The second tie point is the clearly visible ~~the~~ Laacher See Tephra between ~~(~~673 to 680 cm core depth ~~;~~ (Fig. 2A and D) ~~is clearly visible~~. The latter can be used as chronological marker due to the varve counted age of 12,880 a BP in the adjacent Meerfelder Maar (Fig. ~~2C~~A and D; Brauer et al., 1999). ~~The second tie point to establish a chronology for the Lake Gemündener Maar core is a radiocarbon-dated piece of charcoal in 727 cm core depth, which dated to 13,800 ± 110 cal a BP (Fig. 2C). This age is derived from a ^{14}C age of 11,950 ± 65 a BP as part of the supplement material of Sirocko et al. (2013), calibrated using CalPal-software (Weninger and Jöris, 2008) calculated with the IntCal13 calibration curve (Reimer et al., 2013). The uncertainty of the calibrated ^{14}C age represents the 68% probability range.~~ The onset of the Younger Dryas period was set to 12,680 a BP (varve counted in Lake Meerfelder Maar sediments; Brauer et al., 1999; Litt et al., 2009) identified in a depth of 670 cm in the GM1 core due to a clear color change (Fig. 2A and D). The onset of the Preboreal (Holocene) was found to date to 11,590 a BP in Lake Meerfelder Maar by varve counting (Litt et al., 2009) ~~in the Greenland NGRIP core, dated to 11,650 a BP (Walker et al., 2009)~~, This was ~~is~~ used ~~as~~ to wiggle match ~~due~~ the ~~to the~~ distinct changes in the pollen spectra (decreasing *Poaceae*, peaking *Artemisia*, increasing *Pinus* and *Betula*; Fig. 2B and C), the clear rise in TOC (Fig. 3A) and the color change (Fig. 2A), which were identified in 646~~3~~ cm depth ~~TOC increase in 642 cm depth of the Gemündener Maar core~~ (Fig. ~~2A~~2B, ~~C and~~ D). The Late Glacial to Preboreal (Holocene) transition is commonly well recorded in maar sediments from the Eifel region, i.e. clear changes in deposition as well as pollen pattern (Brauer et al., 1999; Litt et al., 2001, 2003; Litt and Stebich, 1999), dated e.g. in Lake Holzmaar to ~~varve counted to~~ 11,600 a BP by a combination of varve counting and ^{14}C dating (Zolitschka, 1998) ~~and to 11,590 a BP in Lake the Meerfelder Maar. (Brauer et al., 1999; Litt et al., 2001, 2003; Litt and Stebich, 1999).~~ The last time marker used to constrain the age model is the middle of the sharp increase in *Corylus* (hazel) pollen at 622 cm depth (Fig. B, C and D). We used this sharp increase as marker for the Preboreal to Boreal transition, which is varve counted by Litt et al. (2009) to 10,740 a BP in the Meerfelder Maar sediments. The offset of 60 years to the varve counted

Holzmaar record of Zolitschka (1998), as it is presented by Litt et al. (2009), is within the uncertainty of placing the onset of the Preboreal in the ~~Lake~~ Gemündener Maar *Corylus* curve.

~~Additionally, the clear appearance of *Corylus* Pollen in 620 cm depth (Fig. 2B; derived from unpublished pollen analysis by F. Sirocko) was wiggle matched to the appearance of *Corylus* pollen in the adjacent Lake Holzmaar core, dated to 10,450 a BP (Sirocko et al., 2016). The beginning of the Younger Dryas period was set to 12,680 a BP (200 a after the Laacher See Tephra), according to the findings from Lake Meerfelder Maar (Litt et al., 2001).~~

The investigated core section from 607 cm to 694 cm depth ~~, with regard to the biomarkers,~~ covers therefore the time between ~ 13,~~200~~ 15~~1~~0 a and ~~9,700~~10,13~~9~~40 a BP, i.e. the Allerød, the Younger Dryas, the Preboreal, and the beginning of the Boreal ~~(Fig. 2A and DC)~~, with regard to the biomarkers (Fig. 2A and D). Assuming ~~a~~ constant sedimentation rates between the markers ~~results in~~, an average resolution of ~~58~~ 51 a/cm can be calculated; the minimum and maximum resolution are 19 and ~~164~~ 124 a/cm, respectively. The part above the Laacher See Tephra reveals a lower mean resolution (5~~6~~5 a/cm) than the section below (30 a/cm).

(Fig. 2)

2.~~4~~3 Biomarker and compound-specific isotope analysis

For δ^2H analyses of *n*-alkanes as well as $\delta^{18}O$ analyses of sugars, 59 samples were prepared from 607 cm to 694 cm depth of the ~~Lake~~ Gemündener Maar GM1 core ~~(Fig. 3A and B)~~, in order to cover the core section with already high TOC content and the Late Glacial to Holocene transition (Fig. ~~2A~~2 and 3A~~, C and D~~). *n*-Alkanes were extracted from 1-6 g freeze-dried and grinded samples by microwave extraction at 100°C for 1 h, using 15 ml of solvent (dichloromethane and methanol, in a ratio 9:1). The resultant total lipid extracts were separated over aminopropyl silica gel (Supelco 45 µm) filled pipette columns. Nonpolar compounds (including *n*-alkanes) were eluted with *n*-hexane. The fraction was spiked with a known amount of 5α-androstanone, used as internal standard. Identification and quantification was carried out on an Agilent MS 5975 (EI) interfaced with an Agilent 7890 GC equipped with a 30 m fused silica capillary column (HP5-MS 0.25 mm i.d., 0.25 µm film thickness), and a split/splitless injector operating in splitless mode at 320°C. Carrier gas was helium and the temperature program was 1 min at 50°C, from 50 to 200°C at 30°C min^{-1}, from 200 to 320°C at 7°C min^{-1}, 5 min at 320°C. Data recording comprised the total ion count (scan mode from m/z 40 to m/z 600) and single ion monitoring (m/z 57, 71, 85 and 99). Concentrations were calculated relative

to the internal standard and to an external standard (*n*-C_{21} to *n*-C_{40} alkane mixture, Supelco), injected in different concentrations (40 ng/µl, 4 ng/µl, 1 ng/µl, 0.4 ng/µl).

Prior to compound-specific isotope analyses, the *n*-alkanes were further purified. The nonpolar fractions were passed over a pipette column filled with activated $AgNO_3$ impregnated silica gel and a pipette column filled with zeolite (Geokleen). After drying, the zeolite was removed using hydrofluoric acid and the *n*-alkanes were recovered by liquid-liquid extraction with hexane. The purified *n*-alkane fractions were measured for their compound-specific stable hydrogen isotope composition (δ^2H). The measurements were performed at the Institute of Geography, University of Bern on an IsoPrime 100 IRMS, coupled to an Agilent 7890A GC via a GC5 pyrolysis/combustion interface operating in pyrolysis modus with a Cr (ChromeHD) reactor at 1000°C. Samples were injected with a split/splitless injector. The GC was equipped with 30 m fused silica column (HP5-MS, 0.32 mm inner diameter, 0.25 µm film thickness). The precision was checked by co-analyzing a standard alkane mixture (*n*-C_{27}, *n*-C_{29}, *n*-C_{33}) with known isotope composition (A. Schimmelmann, University of Indiana), injected twice every six runs. The samples were analyzed in threefold repetitions (except from the samples in 622 and 672 cm depth), and the analytical precision was generally better than 5‰. The stable hydrogen isotope compositions are given in the δ-notation ($\delta^2H_{n\text{-alkane}}$) versus Vienna Standard Mean Ocean Water (VSMOW). The H_3^+-correction factor was checked every two days and stayed stable over the course of measurements at 3.14. The $\delta^2H_{n\text{-alkane}}$ values refer to the area weighted mean of the δ^2H values of *n*-alkanes with 27 and 29 carbon atoms (*n*-C_{27}, *n*-C_{29}), respectively, because of their relatively high abundance in the samples (Fig. 4A).

The sample preparation for $\delta^{18}O$ analyses of hemicellulose/polysaccharide-derived sugars followed standard procedures at the Institute of Agronomy and Nutritional Sciences, Soil Biogeochemistry, Martin-Luther-University Halle-Wittenberg, according to the method of Zech and Glaser (2009). The monosaccharide sugars were hydrolytically extracted from samples containing approximately 10 mg total organic carbon with 10 ml of 4 M trifluoroacetic acid at 105°C for 4 h, applying the method described by Amelung et al. (1996). After filtration over glass fibre filters, the extracted sugars were cleaned using XAD-7 (to remove humic-like substances) and Dowex 50WX8 columns (to remove interfering cations). Afterwards, the purified samples were freeze-dried and derivatized by adding methylboronic acid (4 mg in 400 µl pyridine) for 1 h at 60°C ~~(Knapp, 1979)~~. ~~The methylboronic acid derivatization method ensures that the investigated pentoses arabinose and xylose as well as the deoxyhexoses fucose and rhamnose yield only one peak in the chromatograms (Gross and Glaser, 2004).~~

The compound-specific $\delta^{18}O$ measurements were performed using a Trace GC 2000 coupled to a Delta V Advantage IRMS via an ^{18}O-pyrolysis reactor (GC IsoLink) and a ConFlo IV interface (all devices from Thermo Fisher Scientific, Bremen, Germany). Each sample was measured in threefold repetition, embedded in-between co-derivatized sugar standards in various concentrations and known $\delta^{18}O$ values. The $\delta^{18}O$ values of the samples are expressed in δ-notation ($\delta^{18}O_{sugar}$) versus the Vienna Standard Mean Ocean Water (VSMOW). The measured $\delta^{18}O_{sugar}$ values were corrected for drift, amount and area dependency and also for the hydrolytically introduced oxygen atoms that form carbonyl groups with the C1 atoms of the sugar molecules (Zech and Glaser, 2009). Mean standard ~~uncertainties~~ errors for the triplicate measurements of all 59 samples are 0.6‰, 0.7‰ and 0.7‰ for arabinose, fucose and xylose, respectively. The $\delta^{18}O_{sugar}$ values refer to the $\delta^{18}O$ values of the monosaccharides arabinose, fucose and xylose (Fig. 4B). Rhamnose areas, respectively concentrations, were too low for reliable isotope measurements in ~~many~~ most samples.

2.~~5~~4 Conceptual framework ~~for~~ of the coupl~~inged~~ $\delta^2H_{n\text{-alkane}}$ ~~with~~ -$\delta^{18}O_{sugar}$ ~~results~~paleohygrometer approach

The coupled $\delta^2H_{n\text{-alkane}}$-$\delta^{18}O_{sugar}$ paleohygrometer approach was described in detail by Tuthorn et al. (2015) and Zech et al. (2013a). The most fundamental assumption of the approach is that the isotope composition of leaf water can be reconstructed by applying biosynthetic fractionation factors on the measured $\delta^2H_{n\text{-alkane}}$ and $\delta^{18}O_{sugar}$ values (Fig. ~~4~~5). The concept is furthermore based on the observation that the isotope composition of global precipitation plots typically close to the global meteoric water line (GMWL; $\delta^2H_{prec} = 8 \cdot \delta^{18}O_{prec} + 10$; Dansgaard, 1964). In Germany, a local meteoric water line ($LMWL_{Germany}$) slightly deviating from GMWL was described by Stumpp et al. (2014) ($\delta^2H_{prec} = 7.72 \pm 0.13 \cdot \delta^{18}O_{prec} + 4.90 \pm 0.01$; Fig. ~~4~~5), which we used as the baseline for our calculations. The quite similar LMWLs for Trier ($\delta^2H_{prec} = 7.81 \pm 0.08 \cdot \delta^{18}O_{prec} + 5.06 \pm 0.60$) and Koblenz ($\delta^2H_{prec} = 7.80 \pm 0.07 \cdot \delta^{18}O_{prec} + 2.68 \pm 0.53$) as well as the GMWL are additionally displayed in Fig. ~~4~~ 5 for comparison. The local precipitation is the source for soil water and shallow groundwater, which in turn acts as source water for plants. During daytime, however, leaf water is typically ^2H- and ^{18}O-enriched compared to the source water due to evapotranspiration through the stomata~~, plotting therefore right of the GMWL and the LMWLs~~ (Fig. ~~4~~5; Allison et al., 1985; Bariac et al., 1994; Walker and Brunel, 1990). The leaf water reservoir at the evaporative sites achieves quickly steady-state conditions (Allison et al., 1985; Bariac et al., 1994; Gat et al., 2007; Walker and Brunel, 1990)~~, meaning that~~ Thus, the isotope composition of the transpired water vapor is equal to the

isotope composition of the source water utilized by the plants during the transpiration process. The evaporative enrichment of leaf water under steady-state conditions, can be described via a Craig-Gordon model (e.g. Flanagan et al., 1991; Roden and Ehleringer, 1999) by the following expression (e.g. Barbour et al., 2004):

$$\delta_e \approx \delta_s + \varepsilon^* + \varepsilon_k + (\delta_a - \delta_s - \varepsilon_k)\,\frac{e_a}{e_i}, \qquad \text{(Eq. 1)}$$

where δ_e, δ_s and δ_a are the hydrogen and oxygen isotope compositions of leaf water at the evaporative sites, source water and atmospheric water vapor, respectively, ε^* are the equilibrium enrichment expressed as $(1\text{-}1/\alpha_{L/V}) \cdot 10^3$ where $\alpha_{L/V}$ is the equilibrium fractionation between liquid and vapor in ‰, ε_k are the kinetic fractionation parameters for water vapor diffusion from intracellular air space through the stomata and the boundary layer, both for ^2H and ^{18}O, respectively, and e_a/e_i is the ratio of atmospheric vapor pressure to intracellular vapor pressure. When leaf temperature is equal to air temperature, the e_a/e_i ratio represents ~~the relative humidity~~RH of the local atmosphere~~ (RH)~~. If the plant source water and the local atmospheric water vapor are in isotopic equilibrium, the term $\delta_a - \delta_s$ can approximated by $-\varepsilon^*$. Thus. Eq. (1) can be reduced to:

$$\delta_e \approx \delta_s + \left(\varepsilon^* + \varepsilon_k\right)(1 - RH). \qquad \text{(Eq. 2)}$$

The kinetic fractionation parameters (ε_k) are typically related to stomatal and boundary layer resistances with respect to water flux (Farquhar et al., 1989). Since direct measurements of those plant physiological parameters can be hardly assessed in a paleo application we used the kinetic enrichment parameters C_k instead, derived from a more generalized form of the Craig-Gordon model, for describing the kinetic isotope enrichment for ^2H and ^{18}O, respectively, which leads to Eq. (3) (Craig and Gordon, 1965; Gat and Bowser, 1991):

$$\delta_e \approx \delta_s + \left(\varepsilon^* + C_k\right)(1 - RH). \qquad \text{(Eq. 3)}$$

In a δ^2H-$\delta^{18}O$ diagram, the hydrogen and oxygen isotope composition of leaf and source water can be described as a local deuterium-(d-)excess~~deuterium-excess (d)~~ = $\delta^2H - 7.72 \cdot \delta^{18}O$ (Stumpp et al., 2014) in one equation by using the slope of the $LMWL_{Germany}$ (Eq. 4). This approach is comparable to the d~~euterium~~-excess definition from Dansgaard (1964), who used the equation $d = \delta^2H - 8 \cdot \delta^{18}O$ for a measure of the parallel deviation between a given point in the δ^2H-$\delta^{18}O$ diagram to the GMWL.

$$d_e \approx d_s + \left(\varepsilon_2^* - 7.72 \cdot \varepsilon_{18}^* + C_k^2 - 7.72 \cdot C_k^{18}\right)(1 - RH) \qquad \text{(Eq. 4)}$$

Where d_e and d_s are the d~~euterium~~-excess values of the leaf water at the evaporative sites and the source water, respectively, and the equilibrium (ε_2^* and ε_{18}^*) and kinetic enrichment parameters (C_k^2 and C_k^{18}) are expressed for both isotopes. From Eq. (1) to Eq. (4) the primary control of ~~the relative humidity~~ RH on the isotope composition of the leaf water is demonstrated when stomata are open through transpiration. If d_e can be derived from compound specific δ^2H and $\delta^{18}O$ measurements of the *n*-alkane and sugar biomarkers, which derive δ^2H_e and $\delta^{18}O_e$ values for the purpose of calculating d_e values via the equation $d_e = \delta^2H_e - 7.72 \cdot \delta^{18}O_e$, and the d_s can be approximated also from the d~~euterium~~-excess of the $LMWL_{Germany}$ (= 4.9). Accordingly, Eq. (4) can be rearranged in order to calculate ~~relative humidity~~RH of the local atmosphere normalized to leaf temperature as given by Eq. (5) (Hepp et al., 2017; Tuthorn et al., 2015; Zech et al., 2013a):

$$RH \approx 1 - \frac{\Delta d}{\left(\varepsilon_2^* - 7.72 \cdot \varepsilon_{18}^* + C_k^2 - 7.72 \cdot C_k^{18}\right)}, \qquad \text{(Eq. 5)}$$

where Δd is the distance between d_e and d_s, calculated as $\Delta d = d_e - d_s$. Equilibrium fractionation parameters (ε_2^* and ε_{18}^*) are derived from empirical equations of Horita and Wesolowski (1994) with mean daytime growth-period temperature of 14.8°C (from 6 a.m. to 7 p.m. and April to October, derived from the Nürburg-Barweiler station, approx. 25 km northeast of ~~Lake GM~~Gemündener Maar; hourly data from 1995 to 2015 from Deutscher Wetterdienst, 2016). Equilibrium fractionation factors equal 83.8 and 10.15‰ for ^2H and ^{18}O, respectively. The kinetic fractionation parameters (C_k^2 and C_k^{18}) for ^2H and ^{18}O are set to 25.1 and 28.5‰, respectively, according to Merlivat (1978), who reported maximum values during the molecular diffusion process of water through a stagnant boundary layer. The assumption that maximum kinetic fractionation occurs seems to be most suitable for sedimentological application where a signal averaging over decades can be assumed (see above and discussion in Zech et al., 2013a). It should be also noted that ε_k values of broadleaf trees and shrubs over broad climatic conditions are well in the range with used C_k^2 and C_k^{18} values, revealing 23.9 (±0.9) and 26.7‰ (±1.0) for δ^2H and $\delta^{18}O$, respectively (derived from supplementary data of Cernusak et al., 2016).

The nominator of Eq. (5) describes the parallel distance between the d~~euterium~~-excesses of LMWL and leaf water at the evaporative sites which is converted into ~~relative humidity~~RH values, while the denominator is a combination of the slopes of LMWL and the local evaporation line (LEL). This means in turn that the quantification with Eq. (5) is done by obtaining the distance between the source water points, calculated via the intersects between the individual ~~local evaporation lines~~LELs and the $LMWL_{Germany}$, and the leaf water points. The

underlying slope of those LELs can be derived from Eq. (6) via the Craig-Gordon model using the same assumptions as outlined above in a rearranged form (Eq. 6; Zech et al., 2013a). When using the fractionation parameters from above, the slope of the LEL is constant over time, independent from RH and equal to ~ 2.8 (Eq. 6). ~~are~~This is well in agreement with field and laboratory studies (Allison et al., 1985; Bariac et al., 1994; Gat et al., 2007; Tipple et al., 2013; Walker and Brunel, 1990).

$$S_{LEL} = \frac{\delta_e^2 - \delta_s^2}{\delta_e^{18} - \delta_s^{18}} \approx \frac{\varepsilon_2^* + C_k^2}{\varepsilon_{18}^* + C_k^{18}} \quad \text{(Eq. 6)}$$

In order to provide an uncertainty interval in terms of measurement precision covering the ~~Lake~~ Gemündener Maar ~~relative humidity~~RH record, ~~pooled standard errors (SE) of~~we calculated an error propagation for d_e values ~~were used (~~according to Eq. 7, by using the analytical standard errors (SE). ~~) to generate m~~Maximum and minimum values were then applied to ~~for~~ Eq. (5)~~, which~~ resulting in a lower and upper ~~relative humidity~~RH limit (blue shaded area in Fig. 7~~6~~A).

$$SE\ d_e = \sqrt{\left(SE\ \delta^2H_{n\text{-alkane}}\right)^2 + 7.72 \cdot \left(SE\ \delta^{18}O_{sugar}\right)^2} \quad \text{(Eq. 7)}$$

~~**2.5 Monte-Carlo-based correlation analysis**~~

~~In order to account for uncertainties regarding the here established Lake Gemündener Maar Late Glacial to Early Holocene age-depth model (cf. section 2.2), we applied a Monte-Carlo-based correlation analysis to compare more robustly our RH_{dv} record with the IntCal13 ^{14}C production rates (data from Muscheler et al., 2014). This is assessed by varying the onset of *Corylus*, the onset of the Holocene and the charcoal ^{14}C age of the Lake Gemündener Maar core. The Laacher See Tephra is accurately varve counted with an error of ± 40 a (Brauer et al., 1999), which is negligible small compared to the others, and therefore excluded from the variation procedure. The onset of *Corylus* pollen is dated to 10,450 a BP in ~ 8.4 m depth (Sirocko et al., 2016) in the adjacent Lake Holzmaar core. To put an error on this date, four ^{14}C ages derived from twig material of Lake Holzmaar core are used (from the supplements of Sirocko et al. 2013) two above the *Corylus* onset (4.8 m depth: 3560 ± 25 and 3615 ± 30 a BP) and two below (8.5 m depth: 9740 ± 140 and 9670 ± 90 a BP). By using the CalPal-software (Weninger and Jöris, 2008) with the IntCal13 calibration curve (Reimer et al., 2013) these ages were calibrated to 3860 ± 30, 3930 ± 40, 11080 ± 220 and 11000 ± 160 a cal BP. The errors of the calibrated ^{14}C ages refer to the 68% probability range. This gives a mean error for the upper dates of ± 35 a, and ± 190 a for the lower ones. In error propagation we combined both mean~~

~~errors to ± 225 a for the onset of *Corylus* pollen in the Lake Gemündener Maar core. For the onset of the Holocene in the Lake Gemündener Maar sediments, which was defined as wiggle match between the TOC increase in 642 cm depth and the onset of the Holocene in the Greenland NGRIP core (dated to 11,650 a BP Walker et al., 2009), we combined the maximum counting error for the Holocene onset in the NGRIP core of ± 99 a (Walker et al., 2009) together with a potential time lag of 170 a (Rach et al., 2014) to ± 269 a. Such a time lag was detected in sedimentary hydrogen isotope values of aquatic and terrestrial *n*-alkanes from Lake Meerfelder Maar concerning a lag in hydrologic and environmental effects in Western Europe occurring 170 a later compared to Greenland cooling at the GI-1 to GS-1 transition (Rach et al., 2014). Finally, the derived errors for the onset of the Holocene (±269 a), the onset of *Corylus* (±225 a) and the calibrated charcoal ^{14}C age (±110 a) were used in a correlation procedure based on a Monte-Carlo-Simulations (realized in R, version 3.2.2, R Core Team, 2015). In a first mode the time steps were set to 5 a, while the refining, 10 a around the highest correlation coefficient, was done in yearly resolution. This procedure allows deriving optimized ages for those three dates, which in turn enables the calculation of an adjusted age-depth model.~~

3 Results & Discussion

3.1 Source identification of bulk organic matter and of the investigated *n*-alkane and sugar biomarkers

For basic sedimentological characterization, ~~measurements of TC and~~ TOC ~~(both Fig. 2D)~~, ~~T~~N, ~~(Fig. 2E),~~ δ^{15}N ~~(Fig. 2F)~~, $\delta^{13}C_{TC}$ and $\delta^{13}C_{TOC}$ ~~(both Fig. 2G)~~ as well as the TOC/~~T~~N ratio (Fig. ~~2D~~ 3C to ~~H~~H) are displayed from 605 ~~cm~~ to 727 cm depth. ~~TC and~~ TOC values range from ~~0.6 to 20.7% and from~~ 0.6 to 19.7%~~, respectively. Slightly higher TC values compared to TOC can be attributed to the occurrence of carbonate~~. ~~T~~N ~~reveals a~~ ranges from ~~of~~ 0.1 to 1.4% ~~. In general, TOC and TN depth profiles show the same trends~~ (and correlates highly significant~~ly~~ with TOC ~~vs. TN:~~(r = 0.99, p < 0.001, n = 110)~~.,i.e. an increase during the Allerød, lower values during the Younger Dryas, and larger variations during the Preboreal and the Boreal.~~ Higher TOC contents during the Allerød, Preboreal and Boreal ~~are typically linked to~~likely reflect warmer conditions being favorable for terrestrial and aquatic biomass production, whereas ~~the~~ lower TOC values during the Younger Dryas ~~Younger Dryas~~likely reflect less favorable conditions for biomass production and possibly increasing minerogenic sedimentation~~. (e.g. Brauer et al., 1999). Still, the low TOC content during the late Allerød section (below 690 cm) of Lake Gemündener Maar point to a low organic matter production in the lake as well as allochtonous organic matter input.~~ Interestingly, the Late-Glacial-Early

Holocene TOC patterns seem not to be the same for all maar lakes, because the Meerfelder Maar shows a clear TOC two-phasing during the Younger Dryas (Brauer et al., 1999)~~(Brauer et al., 1999)~~ and the Holzmaar is lacking an ~~Also the~~ Allerød ~~sediments of Lake Holzmaar are not characterized by~~ TOC maximum~~a~~ (Lücke et al., 2003). ~~-~~The $\delta^{15}N$ values of the Gemündener Maar record range from 0 to 5‰, showing the maximum and minimum within the Allerød period. $\delta^{13}C_{TC}$ and $\delta^{13}C_{TOC}$ reveal values between -31 to -17‰ and -36 to -24‰, respectively. While $\delta^{13}C_{TC}$ show maximum values in 703 cm depth, $\delta^{13}C_{TOC}$ is decreasing continuously from the beginning to the end of the Allerød, followed by increasing values during the Younger Dryas and the Preboreal/Boreal, interrupted by a short decrease around the beginning of the Holocene. $\delta^{13}C_{TC}$ clearly show the presence of carbonate between 690 cm and 727 cm depth~~, due to the~~ with more positive $\delta^{13}C_{TC}$ values compared to $\delta^{13}C_{TOC}$ values~~, which is however not clear noticeable from the difference between TC and TOC (compare Fig. 2G with 2D)~~. TOC/~~T~~N ratios range from 5 to 16 with the end of the Allerød revealing increasing ratios, while the late Younger Dryas shows slightly decreasing ratios and the Preboreal is marked by the highest ratios.

(Fig. ~~2~~3)

The source of organic matter in lacustrine sediments of small lakes, as one of the most crucial questions and challenges when interpreting organic proxies from lacustrine sedimentary records (Meyers and Ishiwatari, 1993), can either be autochthon (aquatic origin) or allochthon (terrestrial origin). The ~~carbon to nitrogen ratio (~~TOC/N~~C/N~~ ratio~~)~~ and $\delta^{13}C$ values are most common proxies for sedimentary source determination. While non-vascular aquatic organisms often reveal C/N ratios between 4 and 10 (due to low amounts of cellulose and lignin), vascular plants show commonly C/N ratios of 20 and higher (Meyers and Ishiwatari, 1993). ~~A~~A~~Already Prahl et al. (1980) used~~~~ccording~~ fter Meyers (2003), a TOC/N ratio of ~~> 12~~10 is often used as threshold for ~~a dominance of~~identifying aquatic versus terrestrial input (Fig. ~~2H~~3E). ~~The Lake Gemündener Maar samples below 642 cm (onset of the Holocene) show TOC/TN ratios of mostly < 12, pointing to a high aquatic input, whereas in the section above the ratios shift to values > 12, suggesting a partial contribution of terrestrial material (Fig. 2H; Meyers and Ishiwatari, 1993)~~Accordingly, input of terrestrial organic matter increased during the Allerød, decreased during the Younger Dryas and was highest during the Holocene. ~~Lake~~ The Gemündener Maar $\delta^{13}C_{TOC}$ values (Fig. ~~2G~~3D) are well in range ~~with~~ of C_3 land plants and lacustrine algae (Meyers and Lallier-Vergés, 1999)~~. Most likely, no changes between C_3 and~~; evidence for the occurrence of C_4 land plants ~~occurred in Lake Gemündener Maar catchment history, due to the absence of C_4 land plants~~is missing. ~~Thus~~Overall, no clear additional

information about the sedimentary organic matter origin ~~in~~ of the ~~Lake~~ Gemündener Maar sediments can be ~~achieved~~ inferred neither ~~by~~ from $\delta^{13}C_{TOC}$ alone (c.f. Lücke et al., 2003), nor by combining $\delta^{13}C_{TOC}$ with TOC/~~T~~N ratios (c.f. Meyers and Lallier-Vergés, 1999). When considering that both $\delta^{13}C_{TOC}$ and TOC/N values of terrestrial organic matter are additionally affected by mineralization and degradation, resulting in more positive $\delta^{13}C_{TOC}$ values and lower TOC/N ratios (e.g. Zech et al., 2007), a straightforward interpretation of those proxies seems to be challenging. ~~Much less common~~Similarly, $\delta^{15}N$ ~~values~~ has been investigated as proxy for ~~are used to derive information about~~ sedimentary organic matter origin (Meyers and Ishiwatari, 1993; Meyers and Lallier-Vergés, 1999; Wolfe et al., 1999). ~~Source determination using ^{15}N is based on the finding that dissolved nitrate, which is the nitrogen source for aquatic plants, and atmospheric nitrogen, which is the nitrogen source for land plants, largely differ in their isotope ratios (Peterson et al., 1985). For Lake Gemündener Maar, $\delta^{15}N$ values (Fig. 2F) imply more aquatic input below 690 cm depth while above stronger terrestrial imprint is obvious which is in principle resembling the TOC/TN record.~~ However, numerous ~~alternation~~ possibly influencing ~~pathways of sedimentary ^{15}N due to biogeochemical~~ processes~~,~~ like nitrogen uptake by plants, various nitrogen sources, discrimination during denitrification~~,~~ and diagenesis~~,~~ complicate the use of $\delta^{15}N$ as direct source determination proxy. ~~(Altabet et al., 1995; Meyers and Lallier-Vergés, 1999; Wolfe et al., 1999). However, the $\delta^{15}N$ peak in 690 cm depth coincides with a striking brownish layer (Fig. 2A), revealing low C/N ratios. Possible this marks the input of soil material from the catchment, with soils typically being more positive in $\delta^{15}N$ compared to plant material (Natelhoffer and Fry, 1988). Since the origin of the sedimentary organic matter cannot be determined exactly, the Lake Gemündener Maar sedimentary TOC values (Fig. 2D) should also not be over interpreted. Higher TOC contents during the Allerød, Preboreal and Boreal are typically linked to warmer conditions favorable for aquatic biomass production, whereas the lower TOC values during the Younger Dryas are associated with colder and dryer climate with increasing minerogenic sedimentation (e.g. Brauer et al., 1999). Still, the low TOC content during the late Allerød section (below 690 cm) of Lake Gemündener Maar point to a low organic matter production in the lake as well as allochtonous organic matter input. Also the Allerød sediments of Lake Holzmaar are not characterized by TOC maxima (Lücke et al., 2003).~~

Despite the above presented ~~uncertainties~~uncertainties, ~~describing the source of~~concerning the origin of ~~the~~ bulk sedimentary organic matter in ~~Lake~~ the Gemündener Maar ~~sediments using bulk characteristics~~, the origin of the sedimentary biomarkers, namely *n*-alkanes and sugars, needs to be addressed. This is ~~important~~ crucial because aquatic biomarkers

incorporate the isotope composition of lake water, ~~while~~ whereas terrestrial biomarkers incorporate the isotope composition of leaf water (Huang et al., 2004; Kahmen et al., 2013~~a~~; Mügler et al., 2008; Sachse et al., 2004, 2012; Sauer et al., 2001; Tuthorn et al., 2014; Zech et al., 2013b, 2014b). ~~For a successful application of the coupled $\delta^2H_{n\text{-alkane}}$-$\delta^{18}O_{sugar}$ approach, in terms of deriving relative humidity values, the biomarkers have to originate from leaf material of higher terrestrial plants (Hepp et al., 2017; Tuthorn et al., 2015; Zech et al., 2013a).~~ ~~Regarding~~ With regard to the *n*-alkane biomarkers, high amounts of the chain lengths *n*-C_{27} and *n*-C_{29} ~~were detected in~~are characteristic for the ~~Lake~~ Gemündener Maar sediments~~, which enables then robust compound-specific δ^2H measurements afterwards~~. ~~Those homologues originate~~Such patterns are typical~~ly from~~ for epicuticular leaf wax layers of higher terrestrial plants ~~in the catchment~~ (e.g. Eglinton and Hamilton, 1967). ~~The investigated~~With regard to the sugar biomarkers, ~~pattern~~they were previously studied in detail by Hepp et al. (2016)~~,~~. According to the authors' own results and a compilation from the literature (including e.g. Jia et al., 2008; Prietzel et al., 2013; Zech et al., 2012, 2014b), relatively high amounts of ~~showing that~~ arabinose ~~is primarily of~~are a good indicator for a primarily terrestrial origin (higher vascular plants) of the sugars. ~~, whereas fucose and xylose are mostly of aquatic origin (algae). This interpretation was in agreement with (paleo)soil and sediment data compiled from the literature (cf. references in Hepp et al., 2016).~~

~~Finally, it should be clarified if the investigated sedimentary biomarkers are primarily of leaf origin from higher plants in the catchment. While this holds most likely true for the investigated *n*-alkanes, due to their primary source from epicuticular leaf wax layers of higher terrestrial plants, the neutral sugar arabinose is found in leaf, stem and moss material .~~This interpretation is in agreement with the Gemündener Maar being a small lake with densely forested steep crater walls ~~Firstly, high coverage of the catchment by trees is obvious~~ (Fig. 1C)~~. , leading to high degree of leaf litter input in autumn. Secondly, vegetation grown on the maar crater wall is supposed to be the main input of biomass into the lake, which is typical for steeply shored mare lakes, while the shoreline vegetation contribution should be comparable small. Thirdly, an arboreal to nonarboreal pollen ratio of ~ 84, as mean value throughout the investigated core section is reported (derived from unpublished pollen analysis by F. Sirocko).~~ We therefore ~~assume~~ conclude and suggest that arabinose~~,~~ as well as *n*-C_{27} and *n*-C_{29}~~,~~ in our Gemündener Maar record ~~originate~~ are primarily ~~from hemicellulose structures and from epicuticular waxes of tree leaf material, respectively.~~of terrestrial rather than aquatic origin and thus reflect $\delta^2H/\delta^{18}O_{leaf\text{-}water}$ rather than $\delta^2H/\delta^{18}O_{lake\text{-}water}$.

3.2 Reconstructing leaf water isotope composition based on $\delta^2H_{n\text{-alkane}}$ and $\delta^{18}O_{sugar}$

The δ^2H depth profiles reveal variations of -222 to -134‰ and -220 to -147‰ for *n*-C_{27} and *n*-C_{29}, respectively (Fig. ~~3A~~4A). Their δ^2H patterns correlate highly significant with each other ($r = 0.7$, $p < 0.001$, $n = 59$). Weighted mean δ^2H values were calculated using the relative amounts of *n*-C_{27} and *n*-C_{29}. ~~More negative~~The Younger Dryas is characterized by the most negative δ^2H ~~values are obvious during the Younger Dryas~~values (~~~ 17‰ more negative, with a~~ mean of -~~194~~193‰), whereas ~~compared to~~ the Allerød, ~~the (-182‰),~~ Preboreal ~~(-178‰)~~ and the Boreal yielded less negative values ~~((~~-182‰, -178‰ and -171‰, respectively~~), with regard to the weighted mean *n*-alkane depth profile~~. ~~Overall~~ Still, also the Holocene part ~~of the core average at ~ -175‰, where consistently also largest fluctuations are observed (~ 50‰)~~reveals two pronounced δ^2H minima. Overall, our Gemündener Maar $\delta^2H_{n\text{-alkane}}$ resembles very well the close-by Meerfelder Maar δ^2H *n*-C_{29}~~*n-C29*~~ record of Rach et al. (2014).

~~-~~The $\delta^{18}O$ values for arabinose, xylose and fucose range from 28 to 41‰, 26 to 45‰ and 27 to 46‰, respectively (Fig. ~~43~~B). They overall reveal similar trends (arabinose vs. xylose: $r = 0.7$, $p < 0.001$, $n = 59$; arabinose vs. fucose: $r = 0.8$, $p < 0.001$, $n = 59$; xylose vs. fucose: $r = 0.8$, $p < 0.001$, $n = 59$). All sugar records show a clear shift to more positive values at the Younger Dryas ~~to~~ Holocene transition. While xylose and fucose exhibit a change of ~ 8 and ~~6~~7‰, arabinose $\delta^{18}O$ values show a less ~~positive~~ pronounced shift of ~ 3‰ (changes are based on the mean $\delta^{18}O$ values for the Younger Dryas compared to the Preboreal/Boreal period). Xylose is however slightly more negative throughout the Allerød and Younger Dryas compared to arabinose and fucose. Consistently less pronounced changes can be observed for the Allerød-Younger Dryas transition of 1.~~8~~9, 1.~~4~~7 and 0.~~5~~9‰ for xylose, fucose and arabinose, respectively (based on the mean $\delta^{18}O$ values for the Allerød compared to the Younger Dryas). A distinct minimum during the early Preboreal (633 cm depth) characterizes all three $\delta^{18}O$ sugar records.

(Fig. ~~3~~4)

~~When applying the $\delta^2H_{n\text{-alkane}}$-$\delta^{18}O_{sugar}$ paleohygrometer approach to lacustrine sediments, not only the basic origins of the sedimentary biomarkers have to be clarified (cf. section 3.1), but also prerequisite that leaf water isotope composition is recorded in the biomarkers and can thus be reconstructed from them.~~ The isotope composition of leaf wax *n*-alkanes and leaf (hemi-)celluloses from higher plants are known to be strongly related to the water in which they are biosynthesized. They reflect basically the isotope composition of leaf

water during photosynthetic activity (Barbour and Farquhar, 2000; Cernusak et al., 2005; Kahmen et al., 2013a; Sachse et al., 2012). Hence, the isotope signature of the paleo leaf water, $\delta^{18}O_l$ and $\delta^{2}H_l$, respectively, can be reconstructed by using known biosynthetic fractionation factors (Fig. 45; Eq. 8 and 9). For this purpose, fractionation factors of −160‰ for ^{2}H of the *n*-alkanes *n*-C_{27} and *n*-C_{29} (ε^{2}_{bio}; Sachse et al., 2012; Sessions et al., 1999), and +27‰ for ^{18}O ofthe hemicellulose sugar arabinose (ε^{18}_{bio}; Cernusak et al., 2003; Schmidt et al., 2001; Sternberg et al., 1986; Yakir and DeNiro, 1990) are assumedseem to be appropriate (Eq. 8 and 9).

$$\delta^{18}O_l = (\delta^{18}O_{arabinose} - \varepsilon^{18}_{bio})/(1 + \varepsilon^{18}_{bio}/1000) \quad \text{(Eq. 8)}$$

$$\delta^{2}H_l = (\delta^{2}H_{n\text{-alkane}} - \varepsilon^{2}_{bio})/(1 + \varepsilon^{2}_{bio}/1000) \quad \text{(Eq. 9)}$$

Sucrose exported from photosynthesizing leaves was shown to be ~ +27‰ more positive compared to leaf water (e.g. Cernusak et al., 2003). However, also the cellulose biosynthesis is associated with an enrichment of ~ +27‰ compared to the synthesis water, as shown in growth experiments (e.g. Sternberg et al., 1986; Yakir and DeNiro, 1990). This means that the isotope signal from the leaf water incorporated in the transport sugar sucrose can be dampened by oxygen exchange with local synthesis water during (hemi-)cellulose biosynthesis in the sink tissue (e.g. Barbour and Farquhar, 2000). From the study of tree rings, it is known that stem cellulose does not show the full leaf water ^{18}O enrichment signal. Barbour and Farquhar (2000) related this signal damping to the proportion of unenriched source water contributing to the local synthesis water (p_x) and to the proportion of exchangeable oxygen during cellulose synthesis (p_{ex}). Latter The latter is often assumed to be rather constant around 0.40, as estimated from leaf and wood cellulose of *Eucalyptus globulus* and values compiled from literature (Cernusak et al., 2005), meaning that around 40% of the oxygens in the stem cellulose exchanged. Comparison of grasses to the tree stem regarding the signal transfer from leaf water into the (hemi-)cellulose was already reported by Already Helliker and Ehleringer (2002) compared the signal transfer from leaf water to the cellulose of tree stems with the signal transfer occurring in grasses. For a C_4 grass *Cleistogenes squarrosa*, And Liu et al. (2016) presentedreported on a signal damping in the range between 34 and 53%. for the C_4 grass *Cleistogenes squarrosa.* Indeed, studies on leaf material of *Eucalyptus globulus* (Cernusak et al., 2005) and for *Gossypium hirsutum* (Barbour and Farquhar, 2000) report a total damping of 38% during leaf cellulose synthesis. However, already Wang et al. (1998) presented a large range of damping between 4 and 100% for leaf cellulose synthesis (provided in the supplementary material of Cheesman and Cernusak, 2017), based on plant data grown under the same conditions at Jerusalem Botanical Gardens. The signal damping depends also on p_x.

~~Since no direct p_x measurements on dicotyledonous plant leaves are available so far (Liu et al., 2017), no clear conclusion can be drawn about the oxygen signal damping during (hemi-)cellulose synthesis in the leaves of dicotyledonous plants. The signal damping effect described for cellulose synthesis, however, could partially be lost during synthesis of leaf hemicellulose structures. Pentoses, like the hemicellulose-derived arabinose, are biosynthesized via decarboxylation of the carbon at position six (C6) from glucose (Altermatt and Neish, 1956; Burget et al., 2003; Harper and Bar-Peled, 2002). Waterhouse et al. (2013) showed that the oxygens at C6 position in glucose moieties are most strongly affected by the exchange with local water medium of 80%, as indicated by heterotrophic cellulose synthesis. This leads to the approximation that the influence of the source water and the respective oxygen exchange can be considered negligible for leaf arabinose from trees. This is supported by a strong relationship between leaf water and leaf hemicellulose $\delta^{18}O$ values of dicotyledonous plants grown in climate chambers, pointing to a strong incorporation of the leaf water signal into the leaf hemicellulose sugars (Hepp et al., 2018). The reduction of the signal damping does not seem to apply for the respective stem hemicelluloses, with a mean ^{18}O signal damping of ~ 66% (Sternberg, 2014; Zech et al., 2014c) For a C_4 grass *Cleistogenes squarrosa*, Liu et al. (2016) presented a signal damping range between 34 and 53%. Direct p_x measurements in the grass leaf growth-and-differentiation zone of the same C_4 grass reveal values between 0.9 and 1.0 for ^{18}O (Liu et al., 2017). Comparison of grasses to the tree stem regarding the signal transfer from leaf water into the (hemi-)cellulose was already reported by Helliker and Ehleringer (2002).~~

~~A correction seems to be required against the background of~~Fig. ~~3~~4C illustrates that *Poaceae* pollen concentrations ranged between 11 and 33% during the Allerød and ~~Younger Dryas periods in Lake Gemündener Maar sediments (Fig. 3C; derived from unpublished pollen analysis by F. Sirocko)~~the Younger Dryas in the Gemündener Maar record. Hence, a correction for the ^{18}O signal dampening may be requested in order to take these vegetation changes into consideration. A respective correction procedure based on mass balance considerations is given in Eq. (10) in order to adjust $\delta^{18}O_l$ to $\delta^{18}O_l^{\#}$:

$$\delta^{18}O_l^{\#} = \{(\delta^{18}O_l - \delta^{18}O_s)/[f_{non\text{-}grasses} + (1 - 0.4) - f_{non\text{-}grasses} \cdot (1 - 0.4)]\} + \delta^{18}O_s. \quad \text{(Eq. 10)}$$

The correction presented in Eq. (10) is based on assumptions that 40% (0.4) of the leaf water enrichment is lost during hemicellulose biosynthesis of grass leaves, which is well in range with values presented in the literature for cellulose synthesis in tree rings and grasses, respectively (Cernusak et al., 2005; Liu et al., 2016). Furthermore, the *Poaceae* pollen concentration in percentage is used to calculate the fraction of non-grassy pollen [$f_{non\text{-}grasses}$ = (100 – *Poaceae*)/100] corresponding to the non-grassy biomarker contribution, which may serve as

rough approximation. For a paleo application, $\delta^{18}O_s$ remains a priori unknown. Therefore, the intercept between the individual LEL´s (Eq. 6) and the LMWL of Germany were used to generate $\delta^{18}O_s$ values. Note that the signal damping effect described here for cellulose synthesis is likely not fully applicable to our approach using the sugar biomarker arabinose. In fact, pentoses like arabinose are biosynthesized via decarboxylation of the carbon at position six (C6) from glucose (Altermatt and Neish, 1956; Burget et al., 2003; Harper and Bar-Peled, 2002). Waterhouse et al. (2013) showed that the oxygens at C6 position in glucose moieties are most strongly affected by the exchange with local water medium of 80%, as indicated by heterotrophic cellulose synthesis. Thus, arabinose has lost a strongly exchanged (dampened) oxygen and the remaining pentose shows less ^{18}O signal dampening. ~~The overall assumption is still that (hemi-)cellulose is solely biosynthesized from immediate products of photosynthesis. Storage substances like starch indeed contribute to leaf cellulose synthesis (Terwilliger et al., 2001). So far it can only be speculated that this does not significantly influence the strong relationship between (hemi-)cellulose and leaf water (Terwilliger et al., 2002), as appropriate studies are lacking. Leaf water inhomogeneity and sucrose synthesis gradients within leaves could weaken the leaf water to (hemi-)cellulose correlation (Lehmann et al., 2017; Santrucek et al., 2007). Additionally, changes in ^{18}O fractionation (ε^{18}_{bio}) could hamper a robust leaf water reconstruction based on leaf hemicellulose. Sternberg and Ellsworth (2011) showed for heterotrophically generated cellulose a strong temperature dependence of the biosynthetic fractionation factor. A temperature dependency was also found for ε^{18}_{bio} of stem hemicelluloses from dicotyledonous plants, recalculated by Sternberg (2014) based on results from Zech et al. (2014a). In the reply the authors show that rather the ^{18}O leaf water signal damping (p_{ex}), associated with the steam hemicelluloses synthesis, can be related to the temperature growth (Zech et al., 2014c). However, the evaluation of leaf material from the same plants strongly suggests an ^{18}O fractionation factor of around +27‰ (Hepp et al., 2018). This confirms the validity of Eq. (8) in order to derive leaf water from arabinose $\delta^{18}O$ values.~~

~~The climate chamber experiment of Hepp et al. (2018) revealed furthermore a ^{2}H fractionation between long chained *n*-alkanes (*n*-C_{29} and *n*-C_{31}) and leaf water around -156‰. This is well in line with the commonly reported~~With regard to the ε^{2}_{bio} value of −160‰, ~~(Sachse et al., 2012; Sessions et al., 1999) and~~this biosynthetic fractionation factor is confirmed by climate chamber studies of dicotyledonous plants (Kahmen et al., 2011~~b~~, 2013~~a~~; Tipple et al., 2015). However, the latter studies reveal also a range of ~ 35‰, interpreted as species-specific effects during *n*-alkane biosynthesis. Much more pronounced is the difference between dicotyledonous and monocotyledonous C_3 plants regarding the degree to which the leaf water

isotope enrichment is transferred into leaf *n*-alkanes (Gamarra et al., 2016; Kahmen et al., 2013~~a~~). While dicotyledonous plants show signal transfer rates of 96% on average (Kahmen et al., 2013~~a~~), a larger range between 38 and 61% ~~are~~ is found for monocotyledonous plants (Gamarra et al., 2016). The latter imply that 39 to 62% of the ^2H leaf water enrichment is not recorded by the *n*-alkanes of grasses. ~~The outlined discussion lead to the conclusion that δ^2H_l can be reconstructed based on $\delta^2H_{n\text{-alkane}}$ values (using δ^2H of *n*-C_{27} and *n*-C_{29} via Eq. 9). However, a~~Hence, like for $\delta^{18}O$ a correction ~~seems to be required~~may be requested to account for grass-derived *n*-alkanes ~~input, equivalent to Eq. (10)~~:

$$\delta^2H_l^{\#} = \{(\delta^2H_l - \delta^2H_s)/[f_{non\text{-}grasses} + (1 - 0.5) - f_{non\text{-}grasses} \cdot (1 - 0.5)]\} + \delta^2H_s, \quad \text{(Eq. 11)}$$

where δ^2H_l* are the grass corrected δ^2H_l values. The δ^2H_s values and the non-grassy pollen fraction are defined as in Eq. (10). The mass balance correction presented in Eq. (11) is based on assumptions that only 50% of the leaf water enrichment is incorporated by the *n*-alkanes during biosynthesis in grass leaves ~~(based on a mean value calculated from values reported by Gamarra et al., 2016)~~.

~~Besides the discussion about correct and constant biosynthetic fractionation factors and signal damping factors during biosynthesis, the uncorrected δ^2H values of *n*-C_{27} and *n*-C_{29} can be compared to δ^2H results from *n*-C_{29} alkanes extracted from close-by Meerfelder Maar sediments (Rach et al., 2014). This record covers a comparable timespan from 13,100 to 11,000 varve a BP. The Lake Gemündener Maar $\delta^2H_{n\text{-alkane}}$ record resembles the previously presented Lake Meerfelder Maar results with an overall range of 75‰ (13,200 to 9,700 a BP), with ~ -8‰ more negative values in mean during the Younger Dryas compared to the Allerød and a ~ +17‰ shift in average from Younger Dryas to Holocene. The Lake Meerfelder Maar δ^2H *n*-C_{29} values, interpreted as reflecting mainly δ^2H composition of paleo leaf water, reveal a range of 68‰, ~ -8‰ more negative values in mean during the Younger Dryas compared to the Allerød and a Younger Dryas to Holocene shift in average of ~ +19‰ (Rach et al., 2014).~~

In summary, the above outlined discussion ~~results in four different~~allows reconstructing $\delta^2H/\delta^{18}O_{leaf\text{-}water}$ ~~leaf water correction~~(and thus RH results with ~~scenarios as input for~~ Eq. (5)) for four scenarios (see also Tab. 1): (~~1~~i) without signal dampening, (~~2~~ii) with grass-corrected δ^2H values, (~~3~~iii) with grass-corrected $\delta^{18}O$ values and (iv) with grass-corrected δ^2H and $\delta^{18}O$ values.

(Tab. 1)

3.3 Reconstructing relative humidity based on the coupled $\delta^2H_{n\text{-alkane}}$-$\delta^{18}O_{sugar}$ paleohygrometer approach

The biomarker-based leaf water values (δ_l = δ^2H_l, $\delta^{18}O_l$ via Eq. 8 and 9) result in deuterium-excess values of leaf water (d_l), which range ranging between -125 and -30‰ (Fig. 4-5 and 5A6A). This is well within the range as it can be expected. For instance, Voelker et al. (2014) reported on 'deuterium deviations' (calculated as d-excess of leaf water minus 10‰) ranging from 0 to -200‰. And Mayr (2002) conducted climate chamber experiments with *Vicia*, *Brassica* and *Eucalyptus* during his dissertation and measured δ^2H and $\delta^{18}O$ of leaf water ($\delta^{18}O_{leaf\text{-}water}$ and -$\delta^{18}O_{sugars}$ are published in Zech et al. 2014b). Accordingly, d-excess of leaf water ranged from -38 to -171‰ and correlates highly significantly with RH (ranging from 21 to 68%). A clear enrichment is observed compared to the source water signal (d_s), which was set to +4.9‰ as derived from the deuterium-excess of the $LMWL_{Germany}$ (cf. section 2.4; Fig. 4).

(Fig 45)

Using the Gemündener Maar d_l values (and d_s) as input for Eq. (5), relative humidityRH values during daytime and vegetation period (RH_{dv}) can be calculated (scenario 1 in Tab. 1). Reconstructed RH_{dv} values reveal a range from 32 to 82% (Fig. 65B). The error bars covering the Lake Gemündener Maar RH_{dv} record, calculated using pooled d_e standard errors ranging from 3.2 to 44.4‰ according Eq. (7), results in a spanan RH uncertainty range of 1.7 to 23.4%. in relative humidity terms. It should be noted that for two data points (622 and 672 cm depth) only one, instead of three, $\delta^2H_{n\text{-alkane}}$ measurement result is available, avoiding the calculation of pooled d_e standard errors for those. However, these two data points were excluded from the ranges given above. The RH_{dv} record shows distinctly lowerquite large variability with no clear trend during the -Allerød and the first half of the Younger Dryas. The late Younger Dryas, the early and the middle Preboreal are characterized by lower RH values. By contrast, the middle Preboreal reveals the most pronounced RH maximum. relative humidity values during the late Younger Dryas period, early and late Preboreal, while the Allerød, first half of the Younger Dryas, middle Preboreal and the Boreal are characterized by more humid conditions. The plausibility of the reconstructed RH_{dv} values is furthermore confirmed by the comparison to modern RH_{dv} values from the adjacent meteorological station Nürburg-Barweiler (approx. 25 km northeast of Lake GM; Fig. 5C). The mMean reconstructed RH_{dv} values (mean RH_{dv} =is 53% (;-mean RH_{dv} upper limit = 4645%; mean RH_{dv} lower limit = 621%; see section 2.54). For comparison, the modern RH_{dv} value (6 a.m. to 7 p.m. from April to October) from the adjacent meteorological station Nürburg-Barweiler (approx. 25 km northeast of Lake GM; hourly data

from 1995 to 2015 from Deutscher Wetterdienst, 2016) is ~~resembles the modern mean vegetation period (growth time; April to October) daytime (6 a.m. to 7 p.m.) humidity value of~~is 67% (Fig. 6~~5~~B)~~(hourly data from 1995 to 2015 from Deutscher Wetterdienst, 2016)~~. In addition, the range of the reconstructed RH_{dv} values of 50% is well in agreement with ~~in~~ the modern RH_{dv} variability of 45%, within a range of 48% to 93% (definition and meteorological station details as above). ~~The availability of Lake Gemündener Maar *Poaceae* pollen concentrations (Fig. 3C and 5C; derived from unpublished pollen analysis by F. Sirocko) enables calculating three correction leaf water scenarios, which take into account that grass-derived biomarkers are typically less sensitive leaf water recorders (scenarios 2-4 in Tab. 1; cf. 3.2). The effects on the deuterium-excess of leaf water as well as on the corresponding relative humidity values are shown in Fig. 5A and B.~~As proposed in the previous chapter, three correction scenarios can be applied when reconstructing d_l and RH_{dv} values in order to account for ^{2}H and ^{18}O signal dampening occurring in grasses.

(Fig. 6~~5~~)

~~More specifically, t~~Accordingly, the full correction for grass-derived alkane and sugar biomarkers ~~contribution~~ (scenario 4 in Tab. 1) results in 0.0 to ~~-~~6.~~2~~3% (mean ~~-~~1.~~9~~8%) ~~when comparing RH_{dv} to~~lower $RH_{dv}^{\#*}$ values ($RH_{dv}^{\#*}$ in Fig. 6~~5~~B). The~~is corresponding~~ corresponds to $d_l^{\#*}$ ~~value changes range~~decreases of ~~between -11.8 and~~ ~~-~~0.0~~1~~ to -12.0~~11.8~~‰ ($d_l^{\#*}$ in Fig. 6~~5~~A). Such small changes are still far below the pooled analytical standard errors ~~introduced by the measurement errors (Fig. 5A and B).~~. When only ~~grass-corrected arabinose-based δ~~correcting for the ^{18}O signal dampening$_l^{\#}$ ~~values are used, whereas the *n*-alkane δ^2H_l input stays uncorrected~~ (scenario 3 in Tab. 1), d_l values decrease by~~a range of -22.2 to~~ ~~-~~0.~~1~~ 0 to -22.~~2~~7‰, ~~can be obtained in the $d_l^{\#}$ value differences, and the~~ corresponding ~~relative humidity value changes range between~~to RH decreases of ~~-~~0.~~1~~ 0 ~~and~~ to ~~-~~11.~~6~~12.0% ($d_l^{\#}$ and $RH_{dv}^{\#}$ in Fig. 6~~5~~A and B, respectively). ~~, in terms of comparing RH_{dv} to $RH_{dv}^{\#}$. The opposite scenario became obvious when just the *n*-alkane based grass corrected δ^2H_l* values are used to calculate relative humidity values while arabinose based $\delta^{18}O_l$ remains uncorrected~~By contrast, when only correcting for the ^{2}H signal dampening (scenario 2 in Tab. 1)~~. T~~, this leads to 0.~~1~~0 to 10.~~46~~‰ more positive and ~~shifts of~~ 0.0 to 5.~~56~~%~~, when comparing~~ higher RH_{dv} ~~to~~values (d_l* and RH_{dv}* in Fig. 6~~5~~A and B). ~~Indeed, the respective positive d_l* value changes of 0.1 to 10.4‰ are strongly associated to the *Poaceae* pollen concentration. It is therefore clear why the full corrected $RH_{dv}^{\#}$* values differ only minimal from the uncorrected RH_{dv}. Based on that finding, it could be argued~~ Overall, these results suggest that the reconstructed RH_{dv} values ~~derived from δ^2H_l and $\delta^{18}O_l$~~ are ~~relatively robust against grassy biomarker contributions~~not strongly affected

by ^{2}H and ^{18}O signal dampening of grasses. ~~Further implications against a correction arose from the fact that the relative humidity values derived from the coupled $\delta^{2}H_{n\text{-alkane}}$-$\delta^{18}O_{sugar}$ approach are interpreted as reflecting daytime and vegetation period relative humidity (RH_{dv}; Tuthorn et al., 2015). Leaf biomass production in a temperate forest reveals a bimodal distribution regarding the height due to a dense understory vegetation and high leaf production of annually deciduous trees at ground and upper canopy level, respectively (Graham et al., 2014).~~

We are aware, that microclimatic conditions with higher RH values often develop in lower canopy levels of forests (Graham et al., 2014; Parker, 1995). This may result in RH overestimations when applying the coupled $\delta^{2}H_{n\text{-alkane}}$-$\delta^{18}O_{sugar}$ paleohygrometer approach. ~~Moreover, strong gradients in relative humidity can occur in temperate forest ranging from near to saturated conditions (> 95%) close to the ground (< 5 m height) and highly unsaturated conditions (down to ~ 60%) throughout the upper part of the forest (> 5 m height) in a diurnal cycle (Parker, 1995). This suggest that tree leaves are in average build up under lower humidity conditions, compared to the understory (leaf) biomass. With regard to grass-derived *n*-alkane and sugar contributions to the Lake Gemündener Maar $\delta^{2}H$ and $\delta^{18}O$ biomarker records below 642 cm depth, this would suggest a higher impact of the more humid understory signal, what could lead to higher reconstructed relative humidity values when *Poaceae* input is high. This would contradict the applied grass correction (Eq. 10 and 11), which should therefore be even more carefully reviewed in order to avoid an over interpretation of the corrected values.~~However, most leaf biomass is produced in higher canopy levels being exposed to sunlight and free-air RH values. This is in agreement with a study of Zech et al. (2015), who investigated *n*-alkanes in soils of the tropical montane rainforest of Mt. Kilimanjaro. There, *n*-alkanes reflect $\delta^{2}H_{leaf\text{-}water}$ as calculated from free-air RH rather than as calculated from nearly saturated ground-level RH.

~~It is widely accepted that the bulk leaf water is less enriched compared to the leaf water at the evaporative sites (e.g. Allison et al., 1985; Barbour, 2007). Furthermore the simplified Craig-Gordon model to derive RH values (Eq. 5) requires per definition the input of the deuterium-excess of evaporative site leaf water, as outlined in section 2.4 (Flanagan et al., 1991; Roden and Ehleringer, 1999). In order to estimate the effect on the deuterium-excess of differences between Craig-Gordon predicted δ_e (evaporative site leaf water) and measured δ_l (bulk leaf water), deuterium-excess (d_l and d_e) values were calculated for broadleaf trees and shrubs using the supplementary dataset of Cernusak et al. (2016). Using the complete leaf water isotope data of that supplements, which are available for Australia (Kahmen et al., 2013b) and Hawaii (Kahmen et al., 2011a), a deuterium-excess formulation of $d = \delta^{2}H - 6.86 \cdot \delta^{18}O$, based~~

~~on the additional available xylem water isotope data, was found. The thus calculated values average at -88.5 (±35) and -79.6‰ (±29) for d_l and d_e, respectively. This means that in this dataset, d_l is in average 8.9‰ more negative than d_e, with a standard deviation of 16‰. Since it is general accepted that δ_e is more positive compared to δ_l, one would expect d_e to be more negative compared to d_l. Illustrated in a δ^2H-$\delta^{18}O$ diagram, the δ_e should plot further right on a LEL, while the δ_l is assumed to be a mixture plotting therefore closer to the source water, still on the LEL. However, the average difference is still smaller than the mean analytical error of biomarker-derived d_l with 15‰ (see Eq. 7 for calculation). A deuterium-excess correction to account for the difference between d_l and d_e seems therefore not crucial.~~

~~For a successful relative humidity reconstruction, a constant LEL slope is assumed, meaning isotopic equilibrium between plant source water and the local atmospheric water vapor. For giving a estimation weather this assumption is valid here, one should distinguish between isotopic equilibrium between local atmospheric water vapour and local precipitation and that between local atmospheric water vapour and local source water available for plants, while latter is of importance here. Under present-day European climate, close to isotope equilibrium conditions at ground-level temperature between monthly precipitation and atmospheric water vapour can be assumed (Araguás-Araguás et al., 2000; Jacob and Sonntag, 1991), with the exception of snow during winter months (snow preserves isotope signature established high in the clouds, at significantly lower temperatures). However, the source water for plants is mostly a mixture between soil water and shallow groundwater. The isotope composition of deeper soil water horizons and groundwater is constant and close to annual (weighted) mean isotope signature of precipitation (e.g. Herrmann et al., 1987). Therefore, during summer time, when the plants are photosynthetic active, plant source water is in isotope disequilibrium with atmospheric water vapour to which the leaves are exposed.~~A basic assumption of our coupled $\delta^2H_{n\text{-alkane}}$-$\delta^{18}O_{sugar}$ paleohygrometer approach is isotopic equilibrium between plant source water and water vapour. In order to test the robustness of this assumption and respective effects on reconstructed RH values, ~~The impact on the calculated RH values of the possible lack of equilibrium between plant source water (having the expected isotope signature equal to that of annual weighted mean of local precipitation) and the local atmospheric water vapour during vegetation period, was evaluated using the data provided by~~ we used data of Jacob and Sonntag (1991), who measured the isotope composition of precipitation and of atmospheric water vapour in Heidelberg, Germany, during the period 1981 to 1989. The mean difference between annual weighted means of precipitation (≈ plant source water) ~~to~~ and the water vapour, which was calculated as average over the vegetation period

(April-October). The derived ~~is the~~ (apparent fractionation = (ε_{ap})) ~~, was equilibrium fractionation (= ε*) calculated for the vegetation period (April-October)~~ and ~~and the apparent fractionation (ε_{ap}), derived from Jacob and Sonntag (1991) data,~~ amounts to 18.3 and 1.57‰ in average for ^{2}H and ^{18}O, respectively ~~(ε_{ap} is smaller than ε*)~~. ~~This~~ We used this ε_{ap} ~~apparent fractionation was then used~~ in Eq. (1) instead of the difference δ_a - δ_s and recalculated the RH values ~~were recalculated~~. ~~The effect of this replacement, however,~~This recalculation ~~-~~ leads to an average RH change~~s~~ of only -1.7% (±0.9), which is far below the analytical errors of the d~~euterium~~-excess of leaf water. ~~Apart from a potential disequilibrium between the atmospheric water vapor and the source water, also variable air temperatures can alter the LEL slope. However, a temperature change of ± 10°C shift the reconstructed RH_{dv} values just around ± 1%, via slightly different equilibrium fractionation parameters (leading to an LEL slope range from 3.0 to 2.6; cf. section 2.4). This temperature range largely exceed the expected variation throughout the Late Glacial to Early Holocene transition, inferred e.g. from plant-based mean July temperatures from Isarin and Bohncke (1999). This is in line with the previous finding that such temperature changes are negligible for the relative humidity reconstruction compared to the measurement errors of biomarker isotope analyses (cf. Zech et al., 2013a, and discussion therein). Overall, the used LEL slope of 2.8 (Fig. 4), as well as the above presented range for possibly temperature changes, are well in agreement with field and laboratory studies (Allison et al., 1985; Bariac et al., 1994; Gat et al., 2007; Tipple et al., 2013; Walker and Brunel, 1990).~~

~~A further assumption of the presented paleohygrometer approach is that Δd are solely interpreted as the result of leaf water isotope changes and should thus reflect changes in leaf water evaporative enrichment (Hepp et al., 2017; Tuthorn et al., 2015; Zech et al., 2013a). Indeed, the evaporative enrichment of leaf water is strongly driven by the relative air humidity in the direct surrounding of the leaf (e.g. Eq. 3; Cernusak et al., 2016). However, soil water enrichment is not accounted. Generally, soil water enrichment would shift the plant soil water along the soil evaporation line right of the $LWML_{Germany}$, for which our model does not account leading to an underestimation of RH if, in spite of this, the deuterium-excess of the $LMWL_{Germany}$ approximates d_s. Soil water evaporation typically affects only the upper centimeters of the soil (~ 10 cm; Dubbert et al., 2013), while the trees utilize deeper and thus unenriched soil water (Dawson, 1993). Last but not least~~Finally, ~~An additional prerequisite is~~ the stability of the d~~euterium~~-excess and slope of the $LMWL_{Germany}$ through the past needs to be discussed. According to Stumpp et al. (2014), the long-term d~~euterium~~-excess of precipitation ~~values~~ from 28 sites in Germany do~~es~~ not show pronounced relationships to local

climate conditions of the site. All reported values are close to 10‰, which indicates that Atlantic air masses are the main moisture source for Germany (e.g. Rozanski et al., 1993). In addition, the d~~euterium~~-excess ~~in local~~of precipitation from the ~~close-by~~ stations Trier and Koblenz, being close-by to the Gemündener Maar, reveal rather small variability on monthly, annual and long-term basis ~~compared to the pooled standard error of d_i, which averages at 15‰~~. For Trier monthly average~~d~~s d-excess values (March to October) range from 5.3 to 8.7‰~~.~~, ~~annual precipitation~~Annually weighted mean~~s~~ d-excess values range from 1.9 to 10.6‰, and long-term ~~precipitation~~ weighted mean is 6.7‰ (±2.2); for Koblenz the d-excess values range between 2.1 and 6.4‰, 1.4 and 8.7‰, and the long-term weighted mean is 4.1‰ (±1.8) (derived from IAEA/WMO, 2018). Finally, d~~euterium~~-excess variability in Greenland and Antarctic ice-core does not exceed 4‰ over the here relevant time scale (Masson-Delmotte et al., 2005; Stenni et al., 2010). In addition, paleowater samples from Europe suggest that the atmospheric circulation patterns over the European continent were rather constant throughout the past 35,000 years, which also implies that long-term d~~euterium~~-excess of precipitation ~~does~~ did not deviate substantially from the modern value~~s~~ (Rozanski, 1985). In summary, the variations in the slope of the LMWL of Germany are assumed to be rather small over longer timescales.

~~With regard to t~~The detailed discussion~~s~~ in ~~this section~~the above three chapters address numerous uncertainties when using the coupled $\delta^2H_{n\text{-alkane}}$-$\delta^{18}O_{sugar}$ paleohygrometer approach. Conclusively, the reconstructed RH_{dv} history of the Gemündener Maar seems, however, robust enough to infer reliable paleoclimatic/-hydrologic implications~~seems to be suitable for paleoclimate record comparison~~.

3.4 How dry was the Younger Dryas in Western Europe?

While it is well known that the Younger Dryas was a cold spell occurring in the Northern Hemisphere during the Late Glacial (Denton et al., 2010; Heiri et al., 2014; Isarin and Bohncke, 1999), there is much less clear evidence concerning moisture supply/availability and ~~relative humidity~~RH changes during the Younger Dryas. The ~~Lake~~ Gemündener Maar RH_{dv} ~~results~~ record suggests quite some variability but on average ~~relatively humid~~moderate RH_{dv} conditions of ~ 56% ~~at~~ during the end of the Allerød and the first ~~phase~~ half of the Younger Dryas ~~(~ 56%),~~. ~~which are in the sam~~This is within the range ~~as~~ of modern RH_{dv} values (Fig. 6~~5~~B~~; derived from the adjacent meteorological station Nürburg-Barweiler, approx. 25 km northeast of Lake GM; hourly data from 1995 to 2015 from Deutscher Wetterdienst, 2016)~~).

~~This is followed by~~In the second half of the Younger Dryas, a clear RH_{dv} decrease of ~ 11% ~~towards the end of the Younger Dryas, compared to the Allerød and first phase of the Younger Dryas~~occurred (Fig. 7~~6~~A). Such a two phasing of the Younger Dryas has been suggested previously based on multiproxy climate data for western Europe (Isarin et al., 1998). In more detail, Isarin et al. (1998) ~~point to a subdivided Younger Dryas into~~reported on a cold and humid first phase being followed by drier and warmer conditions ~~for western Europe~~. It is moreover speculated that a shift of the mean sea-ice margin during winter in the North Atlantic Ocean slightly to the north could have caused this two phasing. Reduced cyclonic activity and precipitation affected thereby primarily Western Europe because this region was situated at the southern margin of the main storm tracks during the first Younger Dryas period (Isarin et al., 1998). The authors presented also evidence for ~~a~~ the strengthening of the westerly winds in Western Europe as consequence of northwards shifted North Atlantic Ocean sea-ice margin during the late Younger Dryas period. This contradicts, h~~H~~owever, with the interpretation of ~~varve thickness record from Lake~~the Meerfelder Maar sedimentary record. ~~laminated sediments show a distinctive reduction of the sedimentation rates at 12,240 varve a BP, dividing the Younger Dryas in a first phase with thicker varves while the second period is characterized by slightly reduced sedimentation rate (Brauer et al., 1999). T~~Here, the thicker varves during the early Younger Dryas (between 12,680 and 12,240 varve a BP) are used along with geochemical ~~analysis~~ results as indicator for stronger winter winds (Brauer et al., 2008). In line with this, Brauer et al. (1999) interpreted high biogenic opal contents and *P~~r~~ediastrum* remain concentrations during the early Younger Dryas as enhanced aquatic productivity due to an increased nutrient supply caused by soil erosion and the reworking of littoral sediments. The varve formation throughout the second Younger Dryas period (between 12,240 and 11,590 varve a BP) is ~~characterized as~~interpreted to be mainly controlled by snowmelt driven surface runoff (Brauer et al., 1999). Moreover, the authors speculate if during that time the Meerbach creek ~~came into connection with~~began to drain into the Meerfelder Maar, which could be possibly linked to enhanced precipitation amounts. In summary, the interpretations derived from the Younger Dryas sediments of ~~Lake~~ the Meefelder Maar ~~(~~by Brauer et al.~~,~~ (2008, 1999) ~~is~~ seem neither to be ~~not~~ in accordance with the results ~~from~~ of Isarin et al. (1998), ~~as well as~~nor with the established RH_{dv} ~~results~~ record ~~presented here~~of the Gemündener Maar (Fig. 7~~6~~A).

~~Not fully consistent with both outcomes are the continuously dry conditions during the Younger Dryas, as derived from the difference between~~Recently, Rach et al. (2017) reconstructed RH changes and generally dry Younger Dryas climatic conditions by investigating δ^2H of terrestrial- ~~and~~ versus aquatic-derived *n*-alkanes ~~plant-derived *n*-alkane~~

~~δ^2H values extracted~~ (published in Rach et al., 2014) from ~~Lake~~ the Meefelder Maar ~~sediments~~ archive~~(Rach et al., 2014)~~. ~~It should be noted that Rach et al. (2017) used this difference as main input parameter in their dual-biomarker approach. In more detail, the ~ 10% drop of relative humidity changes between the Allerød and the Younger Dryas period is well comparable to the ~ 10% relative humidity difference between the Allerød and the second phase of the Younger Dryas at Lake Gemündener Maar RH_{dv} record (comparisons is based on mean period values). Moreover, the regeneration towards Allerød humidity level around 12,000 a BP, the distinct rise at the end of the Younger Dryas as well as the overall variability obvious in Lake GM reconstructed RH_{dv} values of 50% throughout the Late Glacial to Holocene transition fit well to the relative humidity changes from Lake Meerfelder Maar. Rach et al. (2017) reconstructed a comparable range of ~ 40% throughout the investigated time period covering the Younger Dryas (11,000 to 13,100 varve a BP). However, the continuous dry conditions during the Younger Dryas period reported by Rach et al. (2017, 2014) do not resemble the Lake Gemündener Maar RH_{dv} record.~~ At the current state of research, it can only be speculated about the reasons for this discrepancy with our Gemündener Maar RH record not corroborating an overall dry Younger Dryas. While the uncertainties of the coupled $\delta^2H_{n\text{-alkane}}$-$\delta^{18}O_{sugar}$ paleohygrometer approach were discussed in detail in the previous chapters, according to our opinion the most important uncertainties affecting the dual biomarker approach of Rach et al. (2014, 2017) are the following. ~~Probably some greater extent of lake water enrichment during the late Allerød and the late Younger Dryas extended the difference between terrestrial and aquatic *n*-alkane δ^2H values, leading consequently to an underestimation of the dryness during those periods~~First, lake water is assumed to reflect δ^2H of precipitation. Indeed, Lake Holzmaar, which seems to be comparable to ~~Lake~~ the Meefelder Maar at least for the drainage conditions via one creek, shows a difference of 7.4‰ in δ^2H between inflow and lake water (Sachse et al., 2004). This lake water enrichment is likely to have been variable in the past, especially when including the speculation concerning the drainage of the Meerbach creek during the Younger Dryas (Brauer et al., 1999). Second, *n*-C_{23} is interpreted to be of aquatic origin (from *Potamogeton*) and used for reconstructing $\delta^2H_{lake\text{-}water}$. However, there is increasing evidence that *n*-C_{23} is also of terrestrial origin (Rao et al., 2014). For instance, Aichner et al. (2018) have recently shown for a lake in Poland that *n*-C_{23} is a variable mixture of aquatic and terrestrial origin in those Late Glacial and Early Holocene sediments. And birch as pioneering and one of the dominant tree species during Late Glacial reforestation of Central Europe is known to produce considerable amounts of mid-chain *n*-alkanes (Tarasov et al., 2013). Albeit not included in the latter publication, *n*-C_{23} concentrations of *Betula exilis* and *Betula pendula* reached 653 and even 2323 µg/g in that study. This is highly relevant, because the biosynthetic

fractionation factor of aquatic *n*-alkanes is much smaller than the one of terrestrial *n*-alkanes. Minor changes in the contribution of terrestrial vs. aquatic *n*-alkanes will thus have a considerable impact on the reconstructed δ^2H *n*-C_{23} record and in turn on reconstructed RH values when applying the dual biomarker approach. Finally, it may be noteworthy to acknowledge, that ~~It is moreover shown by~~ Sachse et al. (2004) ~~that~~ found no significant correlation ~~occurs between~~for δ^2H of *n*-C_{23} ~~alkane δ^2H values, between~~and lake water and precipitation along a European lake surface transect. ~~Finally it can be questioned if Lake Meerfelder Maar *n*-C_{23} alkanes solely originate from *Potamogeton* (Rach et al., 2014) with recent publications indicating that *n*-C_{23} is not necessarily interpreted of aquatic origin (Aichner et al., 2018; Rao et al., 2014). Probably some extend could also originate from soil microbes, transported into the lake sediments during the early Younger Dryas due to high erosion rates (Brauer et al., 1999). In summary, this adds uncertainty to the continuous dryness of the Younger Dryas based on the difference between terrestrial and aquatic *n*-alkane δ^2H values (Rach et al., 2014, 2017).~~

~~Similarly, these uncertainties could potentially affect the difference between terrestrial and aquatic *n*-alkane δ^2H values~~Also recently and also applying the dual biomarker approach, Muschitiello et al. (2015) studied Younger Dryas lake sediments from Hässeldala Port ~~Younger Dryas lake sediments from~~in Southern Sweden ~~(Muschitiello et al., 2015)~~. Here, t~~T~~he authors used ~~the approach presented by Rach et al. (2014) with~~ δ^2H ~~values~~ of *n*-C_{21} ~~representative~~ as proxy for lake water, respectively summer precipitation~~., and *n*-C_{27}, *n*-C_{29} and *n*-C_{31} as reflecting leaf water enrichment~~. The calculated difference between terrestrial and aquatic *n*-alkane δ^2H values suggests more humid conditions at the beginning of the Younger Dryas followed by a more or less steady~~ily~~ trend towards drier conditions, peaking around 11,700 a BP (Muschitiello et al., 2015). This would be, ~~however~~within age uncertainties, in line with ~~Lake~~ Gemündener Maar RH_{dv} minimum between ~ 11,700 and 11,900 a BP~~, within age uncertainties of the Lake Gemündener Maar age-depth model~~. Last but not least, Gázquez et al. (2018)~~A recent publication from the Southern Pyrenees, ~~ analyzed~~ing triple oxygen and hydrogen isotopes of gypsum in the Southern Pyrenees and~~to~~ thus reconstructed ~~relative humidity~~RH changes~~., also report~~Again, more humid conditions are reported for~~at~~ the beginning of the Younger Dryas ~~compared to middle and the end of this phase (Gázquez et al., 2018)~~.

(Fig. 7~~6~~)

~~When searching for a~~In search of possible driver*s*/mechanisms for~~of~~ ~~relative humidity~~the observed Gemündener Maar RH_{dv} record ~~changes during the Late Glacial to Early~~

~~Holocene transition, the Lake Gemündener Maar RH_{dv} record can be compared to~~we came across the ^{14}C production and ^{10}Be flux rates (Fig. 7~~6~~B), derived from IntCal13 and the Greenland ice-cores (GRIP, GISP2), respectively (Muscheler et al., 2014). ~~Such~~ These records are commonly ~~known as~~interpreted in terms of solar activity (and thus insolation) ~~proxies~~ changes (Stuiver and Braziunas, 1988; Vonmoos et al., 2006) and reveal striking similarities with o~~. O~~ur Gemündener Maar RH_{dv} record.~~results suggest that~~ For instance, all three records reveal quite high centennial-scale variability during~~the end of~~ the Allerød and the first ~~phase~~ half of the Younger Dryas ~~are characterized by relatively high RH_{dv} and strong centennial-scale variability (Fig. 6A). This coincides with high and strongly variable ^{14}C production and ^{10}Be flux rates~~. ~~The clear drop of the~~Generally low RH_{dv} values ~~towards~~ during the ~~end~~ second half of the Younger Dryas and the Early Preboreal coincide with ~~is also in agreement with a change to a~~ high~~er~~ solar activity, whereas the ~~level. Although RH_{dv} initially recovered slightly at the onset of the Holocene, the Preboreal is mostly a phase of low RH_{dv}. Much higher variability is pronounced than throughout the Younger Dryas. Lowest values are recorded during the late Preboreal (~ 10,600 a BP), which coincide with increased solar activity. However, a short (~300 a) and pronounced phase of very high~~ pronounced RH_{dv} maximum from~~occurred ~~ 11,~~200~~260 to 10~~1~~,~~9050~~050 a BP coincides within age uncertainties with a pronounced solar activity minimum (Fig. 7~~6~~A and B). We dub this wet period the 'Preboreal Humid Phase'~~, which is again accompanied by low solar activity (Fig. 6A and B). The Preboreal Humid Phase~~, which should not be confused with the Preboreal Oscillation (Björck et al., 1997). The Preboreal Oscillation is a short cold event recorded in Greenland ice-cores ~11,400 ka (Rasmussen et al., 2007) and led to more arid conditions at least in the Netherlands according to palynological results (Bos et al., 2007; van der Plicht et al., 2004). These pollen records also show the existence of a pronounced humid phase thereafter, ~~i.e.~~thus corroborating the 'Preboreal Humid Phase'. Widespread glacial advances in the Alps are also attributed to the Preboreal Oscillation (Moran et al., 2016)~~.~~. ~~but~~ However, given the dating uncertainties they may actually rather reflect increased precipitation during the Preboreal Humid Phase.

It should be emphasized, that the described similarities between the ~~Lake~~ Gemündener Maar RH_{dv} record ~~is overall in good agreement with other local and regional paleoclimate reconstructions. The coherence between RH_{dv} and solar activity, in particular during the Younger Dryas and Preboreal Humid Phase, suggests a possible~~and the solar activity records do not allow an *a priori* causality interpretation. It is widely accepted that the Younger Dryas and the Preboreal Oscillation are related to freshwater forcing in the North Atlantic (e.g. Fisher et al., 2002; Murton et al., 2010; Muschitiello et al., 2015). However, the causes and

mechanisms responsible for climate and environmental changes during the rest of Holocene remain vague, and more research including paleoclimate modelling is clearly needed and encouraged to investigate the possible influence of solar activity (Renssen et al., 2007; Rind, 2002). ~~This can also be inferred from the conducted Monte-Carlo-Simulation based correlation procedure between Lake Gemündener Maar RH_{dv} values and the IntCal13 ^{14}C production rates, which gives a maximum correlation coefficient of 0.37. As such, ~ 14% variability in the Lake Gemündener Maar RH_{dv} record can be explained by solar activity changes. This is achieved when the ^{14}C charcoal age, the onset of the Holocene and the onset of *Corylus* pollen were set to 13,716, 11,557 and 10,675 a BP, respectively. However, in terms of deviation to the non-adjusted dates these are changes of +84, +93 and -225 a. The adjustment of the onset of the *Corylus* pollen in Lake Gemündener Maar was therefore set to the maximum oldest age suggesting that for a more detailed driver analysis individual dated climate archives are urgently needed and that the results presented here should not be over interpreted. Apart from these age-depth model uncertainties of the GM,~~ We propose that both the North Atlantic Ocean temperature and solar activity, which triggered solar insolation, were the two main ~~we argue a conceivably~~ driv~~ing mechanism~~ers for the RH_{dv} variability in Central Europe~~ could be a combination of solar activity changes, which triggered solar insolation, and North Atlantic Ocean temperature evolution~~. A key example might be the Preboreal Humid Phase. It can be expected that the North Atlantic Ocean, the main moisture source for Central Europe, revealed already considerably~~e~~ higher temperatures during the Preboreal Humid Phase compared to the Younger Dryas, as indicated by a consistent ~ 2°C increase in planktonic foraminifera (*Globorotalia inflata*, *Globorotalia bulloides* and *Neogloboquadrina pachyderma*) derived Mg/Ca temperatures from a marine sediment core south of Iceland (Fig. 7~~6~~B, Thornalley et al., 2009, 2010, 2011). ~~In summary, t~~This ~~could lead~~led to an enhanced moisture content of the atmosphere. When these wet~~ter~~ air masses were transported onto continental Europe, where low solar insolation inhibited warming up and drying of these air masses, ~~more~~ pronounced humid climate conditions were established. ~~Yet, it can be only speculated if the solar activity minimum during the early Younger Dryas (Fig. 6B) together with strong winds (Brauer et al., 2008) established climatic boundary conditions favoring sea water evaporation, which might have led to increased RH_{dv} in Western Europe (Fig. 6A). Moreover, during the second phase of the Younger Dryas, in which a slight cooling of the North Atlantic Ocean coinciding with increasing solar activity, the climatic conditions on the European continent could have become drier, as suggested by the Lake Gemündener Maar RH_{dv} record. In this light, the applied $\delta^2H_{n\text{-}alkane}$ $\delta^{18}O_{sugar}$ approach has great potential for establishing more quantitative relative humidity records, offering a paleohygrometer approach for better understanding of past climate change.~~

4 Conclusions

Referring to the underlying research questions and based on the presented results and the outlined discussion (including the cited literature) the following conclusions have to be drawn:

- The terrestrial vs. aquatic origin of bulk sedimentary organic matter cannot be determined unambiguously for the Gemündener Maar. This is caused by the bulk proxies (TOC/~~T~~N, $\delta^{13}C$ and $\delta^{15}N$) being not straightforward interpretable. ~~At the same time, this also hampers inferring paleoclimate information based on those proxies.~~ By contrast, the alkane biomarkers with the chain-length *n*-C_{27} and *n*-C_{29} and the sugar biomarker arabinose can be most likely associated with the epicuticular leaf-wax layers and the hemicellulose structures of higher terrestrial plants, respectively. Therefore, they are ~~assumed~~ interpreted to originate primarily from leaf material of the Gemündener Maar catchment~~, which enabled us to use them in the coupled δ^2H-$\delta^{18}O$ paleohygrometer approach~~.
- $\delta^2H/\delta^{18}O_{leaf\text{-}water}$ ~~Leaf water can~~ could be ~~accessed~~ reconstructed from $\delta^2H_{n\text{-alkane}}$ (*n*-C_{27} and *n*-C_{29}) and $\delta^{18}O_{sugar}$ (arabinose) by applying ~~constant~~ biosynthetic fractionation factors. We acknowledge that the assumption of constant fractionation factors introduces ~~considerable uncertainties~~ uncertainty as highlighted by the broad literature discussion. ~~Additionally, a~~A correction for the signal dampening of ~~the reconstructed~~ leaf water ~~isotope composition seems to be required to~~ $^2H/^{18}O$ enrichment ~~account for grassy~~occurring ~~*n*-alkane (*n*-C_{27} and *n*-C_{29}) and arabinose contribution, because~~ in grasses is possible but seems negligible in the case of the Gemündener Maar record~~are known to be less sensitive leaf water enrichment recorders~~.
- The ~~reconstruction of relative humidity values is quite robust; it does not depend strongly on different scenarios used for calculating leaf water values~~detailed discussion of possible uncertainties of the applied coupled $\delta^2H_{n\text{-alkane}}$-$\delta^{18}O_{sugar}$ paleohygrometer approach suggests that robust RH reconstructions are possible for the Gemündener Maar record. ~~Furthermore, a correction to account for possible differences between Craig-Gordon modeled and measured leaf water isotope composition turned out to be dispensable for the here applied paleohyrometer approach. A constant leaf water evaporation line throughout the past seems to be a valid assumption. This was shown by alternative relative air humidity calculations based on apparent fractionation values, which account for a possible lack of equilibrium between plant source water and local~~

~~atmospheric water vapour. The differences to the conventional reconstructed relative air humidity values (via Eq. 5) are far below the analytical errors associated with $\delta^2H_{n\text{-alkane}}$ and $\delta^{18}O_{sugar}$ measurements. Moreover, the used local meteoric water line of Germany seems to be a solid base line here.~~ The reconstructed ~~relative air humidity~~RH values ~~are interpreted to reflect RH of the~~refer to daytime and ~~the~~ vegetation period (RH_{dv}).

- The established ~~Lake~~ Gemündener Maar RH_{dv} record supports a two-phasing of the Younger Dryas~~, i.e. a~~ with moderate wet conditions on Allerød level during the first half and drier conditions during the second half of the Younger Dryas ~~relative wet phase on Allerød level followed by a drier Younger Dryas ending~~. Overall dry~~ier~~ climatic conditions ~~throughout~~ characterizing the Younger Dryas ~~or a two-phasing in terms of a first dry and cold Younger Dryas phase followed by a warmer period along with increasing precipitation amounts~~ could not be corroborated. ~~Surprisingly~~Unexpectedly, the amplitude of RH_{dv} changes during the Early Holocene was more pronounced ~~compared to~~than during the Younger Dryas and includes a pronounced 'Preboreal Humid Phase' occurring from ~11,2~~0~~60 to 1~~0~~1,9~~50~~050 a BP. ~~One possible driver for the unexpected Lake Gemündener Maar RH_{dv} variations could be the solar activity, as derived from the comparison with IntCal ^{14}C production and Greenland ice-core ^{10}Be flux rate data.~~We propose North Atlantic Ocean temperature and solar activity (and thus insolation) to be the main drivers for Late Glacial-Early Holocene RH changes in Central Europe and encourage respective paleoclimate modelling studies in order to validate or falsify our proposition.

Data availability

The data ~~will be made available upon request~~is available via the supplementary data file.

Author contributions

J. Hepp ~~and,~~ L. Wüthrich and M. Zech wrote the ~~paper~~manuscript; M. Zech and R. Zech acquired financial support ~~and wrote the paper~~. F. Sirocko was responsible for lake coring and provided the chronology and stratigraphy. L. Wüthrich, J. Hepp, T. Bromm, M. Bliedtner and I.K. Schäfer carried out laboratory work and did data evaluation. M. Bliedtner, I.K. Schäfer, B. Glaser, K. Rozanski, F. Sirocko and R. Zech contributed to the discussion of the data and commented on the manuscript.

Competing interests

Competing financial interests: The authors declare no competing financial interests.

Acknowledgements

We greatly acknowledge R. Muscheler (Lund University) for providing ^{10}Be flux as well as ^{14}C production rates data. We thank M. Benesch (Martin-Luther-University Halle-Wittenberg), A. Kühnel (Technical University of Munich), J. Zech (University of Bern), F. Dreher (Johannes Gutenberg University of Mainz), S. Lutz (University of Zurich), N. Baltić and P. Kretschmer (Martin-Luther-University Halle-Wittenberg) for their support during laboratory work and statistical analyses. We cordially thank P.M. Grootes (Kiel University) for valuable recommendations during manuscript preparation and K. Mills, P.A. Meyers and an anonymous reviewer for their great editorial support and constructive and encouraging reviews. Our paper also greatly profited from short comments provided by B. Zolitschka, A. Lücke, E. Schefuß, D. Sachse and F. Schenk (see SCs on discussion paper and our replies). ~~A. Kühnel (Technical University of Munich) for helping us in establishing the Monte-Carlo-based correlation scheme~~. Swiss National Science Foundation (PP00P2 150590) fundeds ~~L~~ L. Wüthrich, M. Bliedtner, I.K. Schäfer and R. Zech. Involvement of K. Rozanski was supported by AGH UST statutory task No. 11.11.220.01/1 within subsidy of the Ministry of Science and Higher Education. J. Hepp greatly acknowledges the support given by the German Federal Environmental Foundation.

References

Aichner, B., Ott, F., Słowiński, M., Noryśkiewicz, A. M., Brauer, A. and Sachse, D.: Leaf wax *n*-alkane distributions record ecological changes during the Younger Dryas at Trzechowskie paleolake (Northern Poland) without temporal delay, Climate of the Past Discussions, (March), 1–29, doi:10.5194/cp-2018-6, 2018.

Alley, R. B.: The Younger Dryas cold interval as viewed from central Greenland, Quaternary Science Reviews, 19(1–5), 213–226, doi:10.1016/S0277-3791(99)00062-1, 2000.

Allison, G. B., Gat, J. R. and Leaney, F. W. J.: The relationship between deuterium and oxygen-18 delta values in leaf water, Chemical Geology, 58, 145–156, 1985.

Altermatt, H. A. and Neish, A. C.: The biosynthesis of cell wall carbohydrates: III. Further studies on formation of cellulose and xylan from labeled monosaccharides in wheat plants, Canadian Journal of Biochemistry and Physiology, 34(3), 405–413, doi:10.1139/o56-042, 1956.

Amelung, W., Cheshire, M. V. and Guggenberger, G.: Determination of neutral and acidic sugars in soil by capillary gas-liquid chromatography after trifluoroacetic acid hydrolysis, Soil Biology and Biochemistry, 28(12), 1631–1639, 1996.

Araguás-Araguás, L., Froehlich, K. and Rozanski, K.: Deuterium and oxygen-18 isotope composition of precipitation and atmospheric moisture, Hydrological Processes, 14(8), 1341–1355, doi:10.1002/1099-1085(20000615)14:8<1341::AID-HYP983>3.0.CO;2-Z, 2000.

Barbour, M. M. and Farquhar, G. D.: Relative humidity-and ABA-induced variation in carbon and oxygen isotope ratios of cotton leaves, Plant, Cell & Environment, 23(5), 473–485, 2000.

Barbour, M. M., Roden, J. S., Farquhar, G. D. and Ehleringer, J. R.: Expressing leaf water and cellulose oxygen isotope ratios as enrichment above source water reveals evidence of a Péclet effect, Oecologia, 138(3),

426–435, doi:10.1007/s00442-003-1449-3, 2004.
Bariac, T., Gonzalez-Dunia, J., Katerji, N., Béthenod, O., Bertolini, J. M. and Mariotti, A.: Spatial variation of the isotopic composition of water (^{18}O, ^{2}H) in the soil-plant-atmosphere system, 2. Assessment under field conditions, Chemical Geology, 115, 317–333, 1994.
Björck, S., Rundgren, M., Ingólfsson, O. and Funder, S.: The Preboreal oscillation around the Nordic Seas: terrestrial and lacustrine responses, Journal of Quaternary Science, 12(6), 455–465, doi:10.1002/(SICI)1099-1417(199711/12)12, 1997.
Bos, J. A. A., van Geel, B., van der Plicht, J. and Bohncke, S. J. P.: Preboreal climate oscillations in Europe: Wiggle-match dating and synthesis of Dutch high-resolution multi-proxy records, Quaternary Science Reviews, 26(15–16), 1927–1950, doi:10.1016/j.quascirev.2006.09.012, 2007.
Brauer, A., Endres, C., Günter, C., Litt, T., Stebich, M. and Negendank, J. F. W.: High resolution sediment and vegetation responses to Younger Dryas climate change in varved lake sediments from Meerfelder Maar, Germany, Quaternary Science Reviews, 18(3), 321–329, doi:10.1016/S0277-3791(98)00084-5, 1999.
Brauer, A., Haug, G. H., Dulski, P., Sigman, D. M. and Negendank, J. F. W.: An abrupt wind shift in western Europe at the onset of the Younger Dryas cold period, Nature Geoscience, 1(8), 520–523, doi:10.1038/ngeo263, 2008.
Brunck, H., Sirocko, F. and Albert, J.: The ELSA-Flood-Stack: A reconstruction from the laminated sediments of Eifel maar structures during the last 60,000 years, Global and Planetary Change, 142, 136–146, doi:10.1016/j.gloplacha.2015.12.003, 2015.
Büchel, G.: Maars of the Westeifel, Germany, in Paleolimnology of European Maar Lake, vol. 49, edited by L. Negendank and B. Zolitschka, pp. 1–13, Springer-Verlag, Berlin Heidelberg., 1993.
Büchel, G.: Vulkanologische Karte der West- und Hocheifel 1:50000, Koblenz., 1994.
Burget, E. G., Verma, R., Mølhøj, M. and Reiter, W.-D.: The Biosynthesis of L-Arabinose in Plants: Molecular Cloning and Characterization of a Golgi-Localized UDP-D-Xylose 4-Epimerase Encoded by the MUR4 Gene of Arabidopsis, Plant Cell, 15(February), 523–531, doi:10.1105/tpc.008425.response, 2003.
Cernusak, L. A., Wong, S. C. and Farquhar, G. D.: Oxygen isotope composition of phloem sap in relation to leaf water in Ricinus communis, Functional Plant Biology, 30(10), 1059–1070, 2003.
Cernusak, L. A., Farquhar, G. D. and Pate, J. S.: Environmental and physiological controls over oxygen and carbon isotope composition of Tasmanian blue gum, *Eucalyptus globulus*, Tree Physiology, 25(2), 129–146, doi:10.1093/treephys/25.2.129, 2005.
Cernusak, L. A., Barbour, M. M., Arndt, S. K., Cheesman, A. W., English, N. B., Feild, T. S., Helliker, B. R., Holloway-Phillips, M. M., Holtum, J. A. M., Kahmen, A., Mcinerney, F. A., Munksgaard, N. C., Simonin, K. A., Song, X., Stuart-Williams, H., West, J. B. and Farquhar, G. D.: Stable isotopes in leaf water of terrestrial plants, Plant Cell and Environment, 39(5), 1087–1102, doi:10.1111/pce.12703, 2016.
Craig, H. and Gordon, L. I.: Deuterium and oxygen-18 variations in the ocean and the marine atmosphere, in Proceedings of a Conference on Stable Isotopes in Oceanographic Studies and Palaeotemperatures, edited by E. Tongiorgi, pp. 9–130, Lischi and Figli, Pisa., 1965.
Dansgaard, W.: Stable isotopes in precipitation, Tellus, 16(4), 436–468, doi:10.1111/j.2153-3490.1964.tb00181.x, 1964.
Denton, G. H., Anderson, R. F., Toggweiler, J. R., Edwards, R. L., Schaefer, J. M. and Putnam, A. E.: The Last Glacial Termination, Science, 328(5986), 1652–1656, doi:10.1126/science.1184119, 2010.
Deutscher Wetterdienst: Climate data center, Nürburg-Barweiler station [online] Available from: ftp://ftp-cdc.dwd.de/pub/CDC/ (Accessed 10 August 2016), 2016.
Eglinton, G. and Hamilton, R. J.: Leaf Epicuticular Waxes, Science, 156(3780), 1322–1335, doi:10.1126/science.156.3780.1322, 1967.
Farquhar, G. D., Hubick, K. T., Condon, A. G. and Richards, R. A.: Carbon Isotope Fractionation and Plant Water-Use Efficiency, in Stable Isotopes in Ecological Research. Ecological Studies (Analysis and Synthesis), vol. 68, edited by P. W. Rundel, J. R. Ehleringer, and K. A. Nagy, pp. 21–40, Springer-Verlag, New York., 1989.
Fisher, T. G., Smith, D. G. and Andrews, J. T.: Preboreal oscillation caused by a glacial Lake Agassiz flood, Quaternary Science Reviews, 21(8–9), 873–878, doi:10.1016/S0277-3791(01)00148-2, 2002.
Flanagan, L. B., Comstock, J. P. and Ehleringer, J. R.: Comparison of Modeled and Observed Environmental Influences on the Stable Oxygen and Hydrogen Isotope Composition of Leaf Water in Phaseolus vulgaris L., Plant Physiology, (96), 588–596, 1991.
Gamarra, B., Sachse, D. and Kahmen, A.: Effects of leaf water evaporative ^{2}H-enrichment and biosynthetic fractionation on leaf wax *n*-alkane $\delta^{2}H$ values in C3 and C4 grasses, Plant, Cell and Environment Environment, 39, 2390–2403, doi:10.1111/pce.12789, 2016.
Gat, J. R. and Bowser, C. J.: The heavy isotope enrichment of water in coupled evaporative systems, in Stable Isotope Geochemistry: A Tribute to Samuel Epstein, vol. 3, edited by H. P. Tayler, J. R. O'Neil, and I. R. Kaplan, pp. 159–168, The Geochemical Society, Lancester., 1991.
Gat, J. R., Yakir, D., Goodfriend, G., Fritz, P., Trimborn, P., Lipp, J., Gev, I., Adar, E. and Waisel, Y.: Stable

isotope composition of water in desert plants, Plant and Soil, 298(1--2), 31–45, doi:10.1007/s11104-007-9321-6, 2007.

Gázquez, F., Morellón, M., Bauska, T., Herwartz, D., Surma, J., Moreno, A., Staubwasser, M., Valero-Garcés, B., Delgado-Huertas, A. and Hodell, D. A.: Triple oxygen and hydrogen isotopes of gypsum hydration water for quantitative paleo-humidity reconstruction, Earth and Planetary Science Letters, 481, 177–188, doi:10.1016/j.epsl.2017.10.020, 2018.

Graham, H. V, Patzkowsky, M. E., Wing, S. L., Parker, G. G., Fogel, M. L. and Freeman, K. H.: Isotopic characteristics of canopies in simulated leaf assemblages, Geochimica et Cosmochimica Acta, 144, 82–95, doi:10.1016/j.gca.2014.08.032, 2014.

Harper, A. D. and Bar-Peled, M.: Biosynthesis of UDP-Xylose. Cloning and Characterization of a Novel Arabidopsis Gene Family, UXS, Encoding Soluble and Putative Membrane-Bound UDP-Glucuronic Acid Decarboxylase Isoforms, Gene, 130(December), 2188–2198, doi:10.1104/pp.009654.2188, 2002.

Heiri, O., Koinig, K. A., Spötl, C., Barrett, S., Brauer, A., Drescher-Schneider, R., Gaar, D., Ivy-Ochs, S., Kerschner, H., Luetscher, M., Moran, A., Nicolussi, K., Preusser, F., Schmidt, R., Schoeneich, P., Schwörer, C., Sprafke, T., Terhorst, B. and Tinner, W.: Palaeoclimate records 60-8 ka in the Austrian and Swiss Alps and their forelands, Quaternary Science Reviews, 106(December), 186–205, doi:10.1016/j.quascirev.2014.05.021, 2014.

Helliker, B. R. and Ehleringer, J. R.: Grass blades as tree rings: environmentally induced changes in the oxygen isotope ratio of cellulose along the length of grass blades, New Phytologist, 155, 417–424, 2002.

Henderson, A. K., Nelson, D. M., Hu, F. S., Huang, Y., Shuman, B. N. and Williams, J. W.: Holocene precipitation seasonality captured by a dual hydrogen and oxygen isotope approach at Steel Lake, Minnesota, Earth and Planetary Science Letters, 300(3--4), 205–214, doi:http://dx.doi.org/10.1016/j.epsl.2010.09.024, 2010.

Hepp, J., Tuthorn, M., Zech, R., Mügler, I., Schlütz, F., Zech, W. and Zech, M.: Reconstructing lake evaporation history and the isotopic composition of precipitation by a coupled $\delta^{18}O$–$\delta^{2}H$ biomarker approach, Journal of Hydrology, 529, 622–631, 2015.

Hepp, J., Rabus, M., Anhäuser, T., Bromm, T., Laforsch, C., Sirocko, F., Glaser, B. and Zech, M.: A sugar biomarker proxy for assessing terrestrial versus aquatic sedimentary input, Organic Geochemistry, 98, 98–104, doi:10.1016/j.orggeochem.2016.05.012, 2016.

Hepp, J., Zech, R., Rozanski, K., Tuthorn, M., Glaser, B., Greule, M., Keppler, F., Huang, Y., Zech, W. and Zech, M.: Late Quaternary relative humidity changes from Mt. Kilimanjaro, based on a coupled ^{2}H-^{18}O biomarker paleohygrometer approach, Quaternary International, 438, 116–130, doi:10.1016/j.quaint.2017.03.059, 2017.

Horita, J. and Wesolowski, D. J.: Liquid-vapor fractionation of oxygen and hydrogen isotopes of water from the freezing to the critical temperature, Geochimica et Cosmochimica Acta, 58(16), 3425–3437, doi:http://dx.doi.org/10.1016/0016-7037(94)90096-5, 1994.

Hou, J., D'Andrea, W. J. and Huang, Y.: Can sedimentary leaf waxes record D/H ratios of continental precipitation? Field, model, and experimental assessments, Geochimica et Cosmochimica Acta, 72, 3503–3517, doi:10.1016/j.gca.2008.04.030, 2008.

Huang, Y., Shuman, B., Wang, Y. and Iii, T. W.: Hydrogen isotope ratios of individual lipids in lake sediments as novel tracers of climatic and environmental change: a surface sediment test, Journal of Paleolimnology, 31, 363–375, 2004.

IAEA/WMO: Global Network of Isotopes in Precipitation. The GNIP Database, [online] Available from: https://nucleus.iaea.org/wiser (Accessed 9 February 2018), 2018.

Isarin, R. F. B. and Bohncke, S. J. P.: Mean July Temperatures during the Younger Dryas in Northwestern and Central Europe as Inferred from Climate Indicator Plant Species, Quaternary Research, 51(02), 158–173, doi:10.1006/qres.1998.2023, 1999.

Isarin, R. F. B., Renssen, H. and Vandenberghe, J.: The impact of the North Atlantic Ocean on the Younger Dryas climate in northwestern and central Europe, Journal of Quaternary Science, 13(5), 447–453, doi:10.1002/(sici)1099-1417(1998090)13:5<447::aid-jqs402>3.0.co;2-b, 1998.

Jacob, H. and Sonntag, C.: An 8-year record of the seasonal- variation of ^{2}H and ^{18}O in atmospheric water vapor and precipitation at Heidelberg, Tellus, 43B(3), 291–300, 1991.

Jia, G., Dungait, J. A. J., Bingham, E. M., Valiranta, M., Korhola, A. and Evershed, R. P.: Neutral monosaccharides as biomarker proxies for bog-forming plants for application to palaeovegetation reconstruction in ombrotrophic peat deposits, Organic Geochemistry, 39(12), 1790–1799, doi:10.1016/j.orggeochem.2008.07.002, 2008.

Kahmen, A., Dawson, T. E., Vieth, A. and Sachse, D.: Leaf wax *n*-alkane δD values are determined early in the ontogeny of Populus trichocarpa leaves when grown under controlled environmental conditions, Plant, Cell and Environment, 34(10), 1639–1651, doi:10.1111/j.1365-3040.2011.02360.x, 2011.

Kahmen, A., Schefuß, E. and Sachse, D.: Leaf water deuterium enrichment shapes leaf wax *n*-alkane δD values of angiosperm plants I: Experimental evidence and mechanistic insights, Geochimica et Cosmochimica Acta, 111, 39–49, 2013.

Litt, T. and Stebich, M.: Bio- and chronostratigraphy of the lateglacial in the Eifel region, Germany, Quaternary International, 61(1999), 5–16, doi:10.1016/S1040-6182(99)00013-0, 1999.

Litt, T., Brauer, A., Goslar, T., Merkt, J., Balaga, K., Müller, H., Ralska-Jasiewiczowa, M., Stebich, M. and Negendank, J. F. W.: Correlation and synchronisation of Lateglacial continental sequences in northern central Europe based on annually laminated lacustrine sediments, Quaternary Science Reviews, 20, 1233,1249, 2001.

Litt, T., Schmincke, H.-U. and Kromer, B.: Environmental response to climatic and volcanic events in central Europe during the Weichselian Lateglacial, Quaternary Science Reviews, 22, 7–32, 2003.

Litt, T., Schölzel, C., Kühl, N. and Brauer, A.: Vegetation and climate history in the Westeifel Volcanic Field (Germany) during the past 11 000 years based on annually laminated lacustrine maar sediments, Boreas, 38(4), 679–690, doi:10.1111/j.1502-3885.2009.00096.x, 2009.

Liu, H. T., Gong, X. Y., Schäufele, R., Yang, F., Hirl, R. T., Schmidt, A. and Schnyder, H.: Nitrogen fertilization and $\delta^{18}O$ of CO_2 have no effect on ^{18}O-enrichment of leaf water and cellulose in *Cleistogenes squarrosa* (C_4) – is VPD the sole control?, Plant Cell and Environment, 39(12), 2701–2712, doi:10.1111/pce.12824, 2016.

Lücke, A., Schleser, G. H., Zolitschka, B. and Negendank, J. F. W.: A Lateglacial and Holocene organic carbon isotope record of lacustrine palaeoproductivity and climatic change derived from varved lake sediments of Lake Holzmaar, Germany, Quaternary Science Reviews, 22(5–7), 569–580, doi:10.1016/S0277-3791(02)00187-7, 2003.

Luetscher, M., Boch, R., Sodemann, H., Spötl, C., Cheng, H., Edwards, R. L., Frisia, S., Hof, F. and Müller, W.: North Atlantic storm track changes during the Last Glacial Maximum recorded by Alpine speleothems, Nature Communications, 6, 6344, doi:10.1038/ncomms7344, 2015.

Masson-Delmotte, V., Jouzel, J., Landais, A., Stievenard, M., Johnson, S. J., White, J. W. C., Werner, M., Sveinbjornsdottir, A. and Fuhrer, K.: GRIP Deuterium Excess Reveals Rapid and Orbital-Scale Changes in Greenland Moisture Origin, Science, 309, 118–121, doi:10.1126/science.1108575, 2005.

Mayr, C.: Möglichkeiten der Klimarekonstruktion im Holozän mit $\delta^{13}C$- und $\delta^{2}H$-Werten von Baum-Jahrringen auf der Basis von Klimakammerversuchen und Rezentstudien, PhD thesis, Ludwig-Maximilians-Universität München. GSF-Bericht 14/02, 152 pp., 2002.

Merlivat, L.: Molecular diffusivities of $H_2{}^{16}O$, $HD^{16}O$, and $H_2{}^{18}O$ in gases, The Journal of Chemical Physics, 69(6), 2864–2871, doi:http://dx.doi.org/10.1063/1.436884, 1978.

Meyers, P. A.: Applications of organic geochemistry to paleolimnological reconstructions: a summary of examples from the Laurentian Great Lakes, Organic Geochemistry, 34, 261–289, 2003.

Meyers, P. A. and Ishiwatari, R.: Lacustrine organic geochemistry - an overview of indicators of organic matter sources and diagenesis in lake sediments, Organic Geochemistry, 20(7), 867–900, 1993.

Meyers, P. A. and Lallier-Vergés, E.: Lacustrine Sedimentary Organic Matter Records of Late Quaternary Paleoclimates, Journal of Paleolimnology, 21(3), 345–372, doi:10.1023/A:1008073732192, 1999.

Moran, A. P., Ivy-Ochs, S., Vockenhuber, C. and Kerschner, H.: First ^{36}Cl exposure ages from a moraine in the Northern Calcareous Alps, Eiszeitalter und Gegenwart – Quaternary Science Journal, 65(2), 145–155, doi:10.3285/eg.65.2.03, 2016.

Mügler, I., Sachse, D., Werner, M., Xu, B., Wu, G., Yao, T. and Gleixner, G.: Effect of lake evaporation on δD values of lacustrine *n*-alkanes: A comparison of Nam Co (Tibetan Plateau) and Holzmaar (Germany), Organic Geochemistry, 39(6), 711–729, 2008.

Murton, J. B., Bateman, M. D., Dallimore, S. R., Teller, J. T. and Yang, Z.: Identification of Younger Dryas outburst flood path from Lake Agassiz to the Arctic Ocean, Nature, 464(7289), 740–743, doi:10.1038/nature08954, 2010.

Muscheler, R., Adolphi, F. and Knudsen, M. F.: Assessing the differences between the IntCal and Greenland ice-core time scales for the last 14,000 years via the common cosmogenic radionuclide variations, Quaternary Science Reviews, 106, 81–87, doi:10.1016/j.quascirev.2014.08.017, 2014.

Muschitiello, F., Pausata, F. S. R., Watson, J. E., Smittenberg, R. H., Salih, A. A. M., Brooks, S. J., Whitehouse, N. J., Karlatou-Charalampopoulou, A. and Wohlfarth, B.: Fennoscandian freshwater control on Greenland hydroclimate shifts at the onset of the Younger Dryas, Nature Communications, 6, 8939, doi:10.1038/ncomms9939, 2015.

Parker, G. G.: Structure and Mircoclimate of Canopies, in Forest Canopies, edited by M. D. Lowman and N. M. Nadkarni, pp. 73–106, Academic Press, San Diego., 1995.

Partin, J. W., Quinn, T. M., Shen, C.-C., Okumura, Y., Cardenas, M. B., Siringan, F. P., Banner, J. L., Lin, K., Hu, H.-M. and Taylor, F. W.: Gradual onset and recovery of the Younger Dryas abrupt climate event in the tropics, Nature Communications, 6, 8061, doi:10.1038/ncomms9061, 2015.

van der Plicht, J., van Geel, B., Bohncke, S. J. P., Bos, J. A. A., Blaauw, M., Speranza, A. O. M., Muscheler, R. and Björck, S.: The Preboreal climate reversal and a subsequent solar-forced climate shift, Journal of Quaternary Science, 19(3), 263–269, doi:10.1002/jqs.835, 2004.

Prietzel, J., Dechamps, N. and Spielvogel, S.: Analysis of non-cellulosic polysaccharides helps to reveal the history of thick organic surface layers on calcareous Alpine soils, Plant and Soil, 365(1–2), 93–114,

doi:10.1007/s11104-012-1340-2, 2013.
Rach, O., Brauer, A., Wilkes, H. and Sachse, D.: Delayed hydrological response to Greenland cooling at the onset of the Younger Dryas in western Europe, Nature Geoscience, 7(2), 109–112, 2014.
Rach, O., Kahmen, A., Brauer, A. and Sachse, D.: A dual-biomarker approach for quantification of changes in relative humidity from sedimentary lipid D/H ratios, Climate of the Past, 13, 741–757, doi:10.5194/cp-2017-7, 2017.
Rao, Z., Zhu, Z., Jia, G., Henderson, A. C. G., Xue, Q. and Wang, S.: Compound specific δD values of long chain *n*-alkanes derived from terrestrial higher plants are indicative of the δD of meteoric waters: Evidence from surface soils in eastern China, Organic Geochemistry, 40(8), 922–930, doi:http://dx.doi.org/10.1016/j.orggeochem.2009.04.011, 2009.
Rao, Z., Jia, G., Qiang, M. and Zhao, Y.: Assessment of the difference between mid- and long chain compound specific $\delta D_{n\text{-alkanes}}$ values in lacustrine sediments as a paleoclimatic indicator, Organic Geochemistry, 76, 104–117, doi:10.1016/j.orggeochem.2014.07.015, 2014.
Rasmussen, S. O., Andersen, K. K., Svensson, A. M., Steffensen, J. P., Vinther, B. M., Clausen, H. B., Siggaard-Andersen, M.-L., Johnsen, S. J., Larsen, L. B., Dahl-Jensen, D., Bigler, M., Röthlisberger, R., Fischer, H., Goto-Azuma, K., Hansson, M. E. and Ruth, U.: A new Greenland ice core chronology for the last glacial termination, Journal of Geophysical Research: Atmospheres, 111(D6), 1–16, doi:10.1029/2005JD006079, 2006.
Rasmussen, S. O., Vinther, B. M., Clausen, H. B. and Andersen, K. K.: Early Holocene climate oscillations recorded in three Greenland ice cores, Quaternary Science Reviews, 26, 1907–1914, doi:10.1016/j.quascirev.2007.06.015.Abstract, 2007.
Rasmussen, S. O., Bigler, M., Blockley, S. P., Blunier, T., Buchardt, S. L., Clausen, H. B., Cvijanovic, I., Dahl-Jensen, D., Johnsen, S. J., Fischer, H., Gkinis, V., Guillevic, M., Hoek, W. Z., Lowe, J. J., Pedro, J. B., Popp, T., Seierstad, I. K., Steffensen, J. P., Svensson, A. M., Vallelonga, P., Vinther, B. M., Walker, M. J. C., Wheatley, J. J. and Winstrup, M.: A stratigraphic framework for abrupt climatic changes during the Last Glacial period based on three synchronized Greenland ice-core records: Refining and extending the INTIMATE event stratigraphy, Quaternary Science Reviews, 106, 14–28, doi:10.1016/j.quascirev.2014.09.007, 2014.
Reimer, P., Bard, E., Bayliss, A., Beck, J., Blackwell, P., Ramsey, C., Buck, C., Cheng, H., Edwards, R., Friedrich, M., Grootes, P., Guilderson, T., Haflidason, H., Hajdas, I., Hatté, C., Heaton, T., Hoffmann, D., Hogg, A., Hughen, K., Kaiser, K., Kromer, B., Manning, S., Niu, M., Reimer, R., Richards, D., Scott, E., Southon, J., Staff, R., Turney, C. and van der Plicht, J.: Intcal13 and Marine13 radiocarbon age calibration curves 0–50,000 years cal BP, Radiocarbon, 55(4), 1869–1887, doi:10.2458/rc.v51i4.3569, 2013.
Renssen, H., Goosse, H. and Fichefet, T.: Simulation of Holocene cooling events in a coupled climate model, Quaternary Science Reviews, 26(15–16), 2019–2029, doi:10.1016/j.quascirev.2007.07.011, 2007.
Rind, D.: The Sun's Role in Climate Variations, Science, 296(5568), 673–677, doi:10.1126/science.1069562, 2002.
Roden, J. S. and Ehleringer, J. R.: Observations of Hydrogen and Oxygen Isotopes in Leaf Water Confirm the Craig-Gordon Model under Wide-Ranging Environmental Conditions, Plant Physiology, 120(August), 1165–1173, 1999.
Rozanski, K.: Deuterium and oxygen-18 in European Groundwaters - Links to Atmospheric Circulation in the Past, Chemical Geology, 52, 349–363, 1985.
Rozanski, K., Araguás-Araguás, L. and Gonfiantini, R.: Isotopic patterns in modern global precipitation, Climate change in continental isotopic records, 1–36, 1993.
Sachse, D., Radke, J. and Gleixner, G.: Hydrogen isotope ratios of recent lacustrine sedimentary *n*-alkanes record modern climate variability, Geochimica et Cosmochimica Acta, 68(23), 4877–4889, doi:http://dx.doi.org/10.1016/j.gca.2004.06.004, 2004.
Sachse, D., Billault, I., Bowen, G. J., Chikaraishi, Y., Dawson, T. E., Feakins, S. J., Freeman, K. H., Magill, C. R., McInerney, F. A., van der Meer, M. T. J., Polissar, P., Robins, R. J., Sachs, J. P., Schmidt, H.-L., Sessions, A. L., White, J. W. C. and West, J. B.: Molecular Paleohydrology: Interpreting the Hydrogen-Isotopic Composition of Lipid Biomarkers from Photosynthesizing Organisms, Annual Reviews, 40, 221–249, doi:10.1146/annurev-earth-042711-105535, 2012.
Sauer, P. E., Eglinton, T. I., Hayes, J. M., Schimmelmann, A. and Sessions, A. L.: Compound-specific D/H ratios of lipid biomarkers from sediments as a proxy for environmental and climatic conditions, Geochimica et Cosmochimica Acta, 65(2), 213–222, doi:http://dx.doi.org/10.1016/S0016-7037(00)00520-2, 2001.
Scharf, B. W. and Menn, U.: Hydrology and morphometry, in In Limnology of Eifel maar lakes, edited by B. Scharf and S. Björk, pp. 43–62, E. Schweizerbart, Stuttgart, Germany., 1992.
Schmidt, H.-L., Werner, R. A. and Roßmann, A.: ^{18}O Pattern and biosynthesis of natural plant products, Phytochemistry, 58(1), 9–32, doi:http://dx.doi.org/10.1016/S0031-9422(01)00017-6, 2001.
Sessions, A. L., Burgoyne, T. W., Schimmelmann, A. and Hayes, J. M.: Fractionation of hydrogen isotopes in lipid biosynthesis, Organic Geochemistry, 30, 1193–1200, 1999.

Sirocko, F., Dietrich, S., Veres, D., Grootes, P. M., Schaber-mohr, K., Seelos, K., Nadeau, M., Kromer, B., Rothacker, L., Röhner, M., Krbetschek, M., Appleby, P., Hambach, U., Rolf, C., Sudo, M. and Grim, S.: Multi-proxy dating of Holocene maar lakes and Pleistocene dry maar sediments in the Eifel , Germany, Quaternary Science Reviews, 62, 56–76, doi:10.1016/j.quascirev.2012.09.011, 2013.

Sirocko, F., Knapp, H., Dreher, F., Förster, M. W., Albert, J., Brunck, H., Veres, D., Dietrich, S., Zech, M., Hambach, U., Röhner, M., Rudert, S., Schwibus, K., Adams, C. and Sigl, P.: The ELSA-Vegetation-Stack: Reconstruction of Landscape Evolution Zones (LEZ) from laminated Eifel maar sediments of the last 60,000 years, Global and Planetary Change, 142, 108–135, doi:10.1016/j.gloplacha.2016.03.005, 2016.

Stenni, B., Masson-Delmotte, V., Selmo, E., Oerter, H., Meyer, H., Röthlisberger, R., Jouzel, J., Cattani, O., Falourd, S., Fischer, H., Hoffmann, G., Iacumin, P., Johnsen, S. J., Minster, B. and Udisti, R.: The deuterium excess records of EPICA Dome C and Dronning Maud Land ice cores (East Antarctica), Quaternary Science Reviews, 29, 146–159, doi:10.1016/j.quascirev.2009.10.009, 2010.

Sternberg, L. S. L., DeNiro, M. J. and Savidge, R. A.: Oxygen Isotope Exchange between Metabolites and Water during Biochemical Reactions Leading to Cellulose Synthesis, Plant Physiology, 82, 423–427, 1986.

Stuiver, M. and Braziunas, T. F.: The Solar Component of the Atmospheric ^{14}C Record, in Secular Solar and Geomagnetic Variations in the Last 10,000 Years, edited by F. R. Stephenson and A. W. Wolfendale, pp. 245–266, Springer, Dordrecht., 1988.

Stumpp, C., Klaus, J. and Stichler, W.: Analysis of long-term stable isotopic composition in German precipitation, Journal of Hydrology, 517, 351–361, doi:10.1016/j.jhydrol.2014.05.034, 2014.

Tarasov, P. E., Müller, S., Zech, M., Andreeva, D., Diekmann, B. and Leipe, C.: Last glacial vegetation reconstructions in the extreme-continental eastern Asia: Potentials of pollen and n-alkane biomarker analyses, Quaternary International, 290–291, 253–263, doi:10.1016/j.quaint.2012.04.007, 2013.

Thornalley, D. J. R., Elderfield, H. and McCave, I. N.: Holocene oscillations in temperature and salinity of the surface subpolar North Atlantic, Nature, 457(7230), 711–714, doi:10.1038/nature07717, 2009.

Thornalley, D. J. R., McCave, I. N. and Elderfield, H.: Freshwater input and abrupt deglacial climate change in the North Atlantic, Paleoceanography, 25(1), 1–16, doi:10.1029/2009PA001772, 2010.

Thornalley, D. J. R., Elderfield, H. and McCave, I. N.: Reconstructing North Atlantic deglacial surface hydrography and its link to the Atlantic overturning circulation, Global and Planetary Change, 79(3–4), 163–175, doi:10.1016/j.gloplacha.2010.06.003, 2011.

Tipple, B. J., Berke, M. A., Doman, C. E., Khachaturyan, S. and Ehleringer, J. R.: Leaf-wax *n*-alkanes record the plant-water environment at leaf flush, Proceedings of the National Academy of Sciences, 110(7), 2659–2664, doi:10.1073/pnas.1213875110, 2013.

Tipple, B. J., Berke, M. A., Hambach, B., Roden, J. S. and Ehleringer, J. R.: Predicting leaf wax *n*-alkane $^{2}H/^{1}H$ ratios: Controlled water source and humidity experiments with hydroponically grown trees confirm predictions of Craig-Gordon model, Plant, Cell and Environment, 38(6), 1035–1047, doi:10.1111/pce.12457, 2015.

Tuthorn, M., Zech, M., Ruppenthal, M., Oelmann, Y., Kahmen, A., del Valle, H. F., Wilcke, W. and Glaser, B.: Oxygen isotope ratios ($^{18}O/^{16}O$) of hemicellulose-derived sugar biomarkers in plants, soils and sediments as paleoclimate proxy II: Insight from a climate transect study, Geochimica et Cosmochimica Acta, 126, 624–634, doi:http://dx.doi.org/10.1016/j.gca.2013.11.002, 2014.

Tuthorn, M., Zech, R., Ruppenthal, M., Oelmann, Y., Kahmen, A., del Valle, H. F., Eglinton, T., Rozanski, K. and Zech, M.: Coupling $\delta^{2}H$ and $\delta^{18}O$ biomarker results yields information on relative humidity and isotopic composition of precipitation - a climate transect validation study, Biogeosciences, 12, 3913–3924, doi:10.5194/bg-12-3913-2015, 2015.

Voelker, S. L., Brooks, J. R., Meinzer, F. C., Roden, J., Pazdur, A., Pawelczyk, S., Hartsough, P., Snyder, K., Plavcova, L. and Santrucek, J.: Reconstructing relative humidity from plant $\delta^{18}O$ and δD as deuterium deviations from the global meteoric water line, Ecological Applications, 24(5), 960–975, doi:10.1890/13-0988.1, 2014.

Voelker, S. L., Stambaugh, M. C., Guyette, R. P., Feng, X., Grimley, D. A., Leavitt, S. W., Panyushkina, I., Grimm, E. C., Marsicek, J. P., Shuman, B. and Brandon Curry, B.: Deglacial hydroclimate of midcontinental North America, Quaternary Research (United States), 83(2), 336–344, doi:10.1016/j.yqres.2015.01.001, 2015.

Volkman, J. K., Barrett, S. M., Blackburn, S. I., Mansour, M. P., Sikes, E. L. and Gelin, F.: Microalgal biomarkers: A review of recent research developments, Organic Geochemistry, 29(5--7), 1163–1179, doi:http://dx.doi.org/10.1016/S0146-6380(98)00062-X, 1998.

Vonmoos, M., Beer, J. and Muscheler, R.: Large variations in Holocene solar activity: Constraints from ^{10}Be in the Greenland Ice Core Project ice core, Journal of Geophysical Research: Space Physics, 111(10), 1–14, doi:10.1029/2005JA011500, 2006.

Wagner, F., Bohncke, S. J. P., Dilcher, D. L., Kürschner, W. M., van Geel, B. and Visscher, H.: Century-Scale Shifts in Early Holocene Atmospheric CO_2 Concentration, Science, 284(June), 1971–1974, 1999.

Walker, C. D. and Brunel, J.-P.: Examining Evapotranspiration in a Semi-Arid Region using Stable Isotopes of

Hydrogen and Oxygen, Journal of Hydrology, 118, 55–75, 1990.

Waterhouse, J. S., Cheng, S., Juchelka, D., Loader, N. J., McCarroll, D., Switsur, V. R. and Gautam, L.: Position-specific measurement of oxygen isotope ratios in cellulose: Isotopic exchange during heterotrophic cellulose synthesis, Geochimica et Cosmochimica Acta, 112(0), 178–191, doi:http://dx.doi.org/10.1016/j.gca.2013.02.021, 2013.

Weninger, B. and Jöris, O.: A ^{14}C age calibration curve for the last 60 ka: the Greenland-Hulu U/Th timescale and its impact on understanding the Middle to Upper Paleolithic transition in Western Eurasia, Journal of Human Evolution, 55(5), 772–781, doi:https://doi.org/10.1016/j.jhevol.2008.08.017, 2008.

Wolfe, B. B., Edwards, T. W. D. and Aravena, R.: Changes in carbon and nitrogen cycling during tree-line retreat recorded in the isotopic content of lacustrine organic matter, western Taimyr Peninsula, Russia, Holocene, 9(2), 215–222, doi:10.1191/095968399669823431, 1999.

Yakir, D. and DeNiro, M. J.: Oxygen and Hydrogen Isotope Fractionation during Cellulose Metabolism in *Lemna gibba* L., Plant Ecology, 93, 325–332, 1990.

Zech, M. and Glaser, B.: Compound-specific $\delta^{18}O$ analyses of neutral sugars in soils using gas chromatography-pyrolysis-isotope ratio mass spectrometry: problems, possible solutions and a first application, Rapid Communications in Mass Spectrometry, 23, 3522–3532, doi:10.1002/rcm, 2009.

Zech, M., Zech, R. and Glaser, B.: A 240,000-year stable carbon and nitrogen isotope record from a loess-like palaeosol sequence in the Tumara Valley, Northeast Siberia, Chemical Geology, 242, 307–318, doi:10.1016/j.chemgeo.2007.04.002, 2007.

Zech, M., Zech, R., Buggle, B. and Zöller, L.: Novel methodological approaches in loess research – interrogating biomarkers and compound-specific stable isotopes, Eiszeitalter und Gegenwart – Quaternary Science Journal, 60(1), 170–187, doi:10.3285/eg.60.1.12, 2011.

Zech, M., Werner, R. A., Juchelka, D., Kalbitz, K., Buggle, B. and Glaser, B.: Absence of oxygen isotope fractionation/exchange of (hemi-) cellulose derived sugars during litter decomposition, Organic Geochemistry, 42(12), 1470–1475, doi:http://dx.doi.org/10.1016/j.orggeochem.2011.06.006, 2012.

Zech, M., Tuthorn, M., Detsch, F., Rozanski, K., Zech, R., Zöller, L., Zech, W. and Glaser, B.: A 220 ka terrestrial $\delta^{18}O$ and deuterium excess biomarker record from an eolian permafrost paleosol sequence, NE-Siberia, Chemical Geology, 360–361, 220–230, doi:http://dx.doi.org/10.1016/j.chemgeo.2013.10.023, 2013a.

Zech, M., Tuthorn, M., Glaser, B., Amelung, W., Huwe, B., Zech, W., Zöller, L. and Löffler, J.: Natural abundance of $\delta^{18}O$ of sugar biomarkers in topsoils along a climate transect over the Central Scandinavian Mountains, Norway, Journal of Plant Nutrition and Soil Science, 176(1), 12–15, doi:10.1002/jpln.201200365, 2013b.

Zech, M., Tuthorn, M., Schlütz, F., Zech, W. and Glaser, B.: A 16-ka $\delta^{18}O$ record of lacustrine sugar biomarkers from the High Himalaya reflects Indian Summer Monsoon variability, Journal of Paleolimnology, 51, 241–251, doi:10.1007/s10933-013-9744-4, 2014a.

Zech, M., Mayr, C., Tuthorn, M., Leiber-Sauheitl, K. and Glaser, B.: Oxygen isotope ratios ($^{18}O/^{16}O$) of hemicellulose-derived sugar biomarkers in plants, soils and sediments as paleoclimate proxy I: Insight from a climate chamber experiment, Geochimica et Cosmochimica Acta, 126(0), 614–623, doi:http://dx.doi.org/10.1016/j.gca.2013.10.048, 2014b.

Zech, M., Zech, R., Rozanski, K., Gleixner, G. and Zech, W.: Do *n*-alkane biomarkers in soils/sediments reflect the $\delta^{2}H$ isotopic composition of precipitation? A case study from Mt . Kilimanjaro and implications for paleoaltimetry and paleoclimate research, Isotopes in Environmental and Health Studies, 51(4), 508–524, doi:10.1080/10256016.2015.1058790, 2015.

Zolitschka, B.: A 14,000 year sediment yield record from western Germany based on annually laminated lake sediments, Geomorphology, 22(1), 1–17, doi:10.1016/S0169-555X(97)00051-2, 1998.

Figures

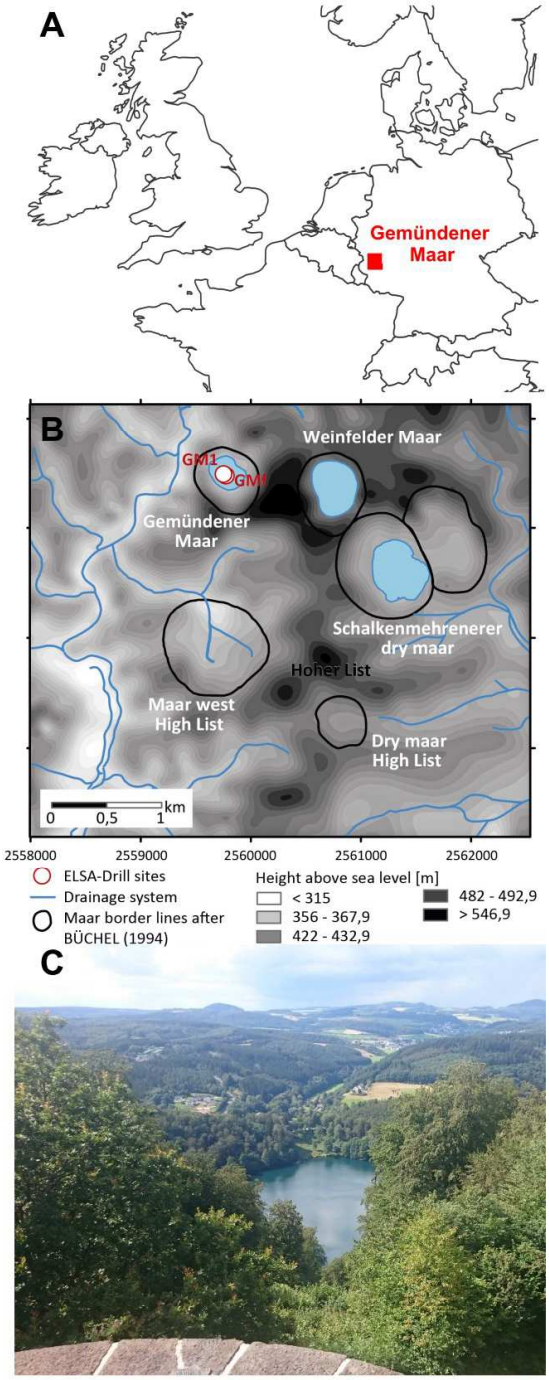

Fig. 1: (A) Location of the ~~Lake~~ Gemündener Maar in the Eifel Region in Germany (generated using OpenStreetMap homepage, www.openstreetmap.org). (B) Digital terrain model and drainage system of the closer surrounding of ~~Lake~~ the Gemündener Maar with maar borders according to Büchel (1994), representing the size of the crater. In addition, the core position is displayed (GM1; 50°10'39.853"N, 6°50'12.912"E) along with the short core GMf (not part of this~~e~~ study) marked as ELSA-Drill sites. Both cores are part of the Eifel Laminated Sediment Archive Project (ELSA-Project). (C) Photo of ~~Lake~~ Gemündener Maar showing the steep and densely ~~vegetated~~ forested catchment (from M. Zech).

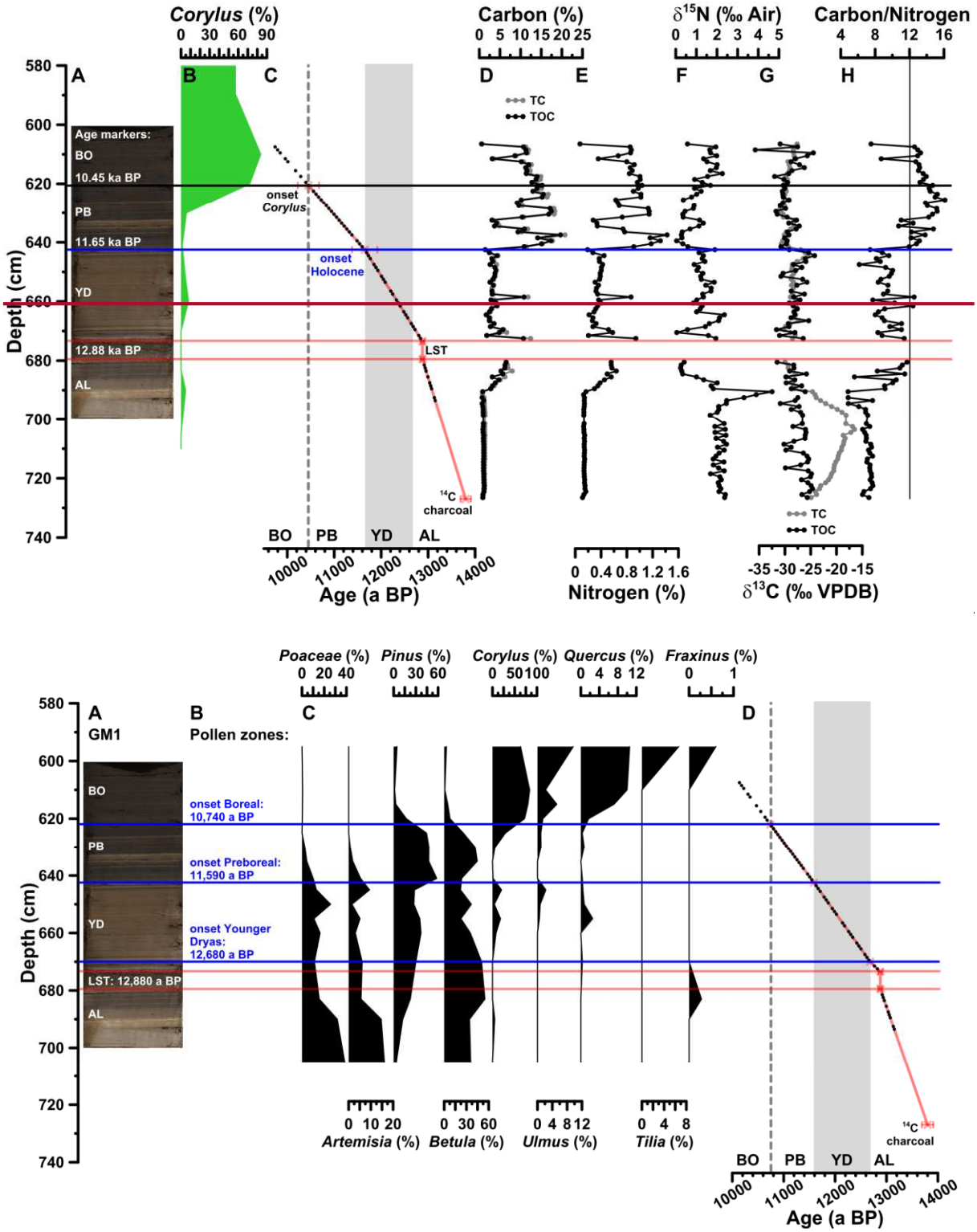

5 **Fig. 2**: (A) Photo of the investigated GM1 core section, with regard to the biomarkers (607 to 694 cm depth), displaying the position of the Laacher See Tephra (LST), varve counted to 12,880 a BP in the adjacent Meerfelder Maar (cf. Brauer et al., 1999)~~including age markers~~.

(B) Defined pollen zones according to Brauer et al. (1999) and Litt et al. (2009). (C) ~~Depth~~ Pollen profiles of pollen groups, which were used for defining the pollen zones. Pollen analysis was realized by F. Dreher (Johannes Gutenberg University of Mainz). ~~*Corylus* pollen (derived from unpublished pollen analysis by F. Sirocko).~~ (~~C~~D) Age-depth model of the full investigated GM1 section (606 to 727 cm depth) consisting of a ^{14}C dated piece of charcoal, the ~~Laacher See Tephra (~~LST~~),~~ and the onsets of the Younger Dryas, Preboreal and Boreal (Holocene~~) (blue line) and *Corylus* pollen (black line)~~. Additionally, the biomarker sampling points ~~(black points)~~ are displayed (black points). The error bars of the ^{14}C age and the LST represent the uncertainty of the calibration (68% probability range) and the error during of the varve counting (± 40 a; Brauer et al., 1999), respectively.

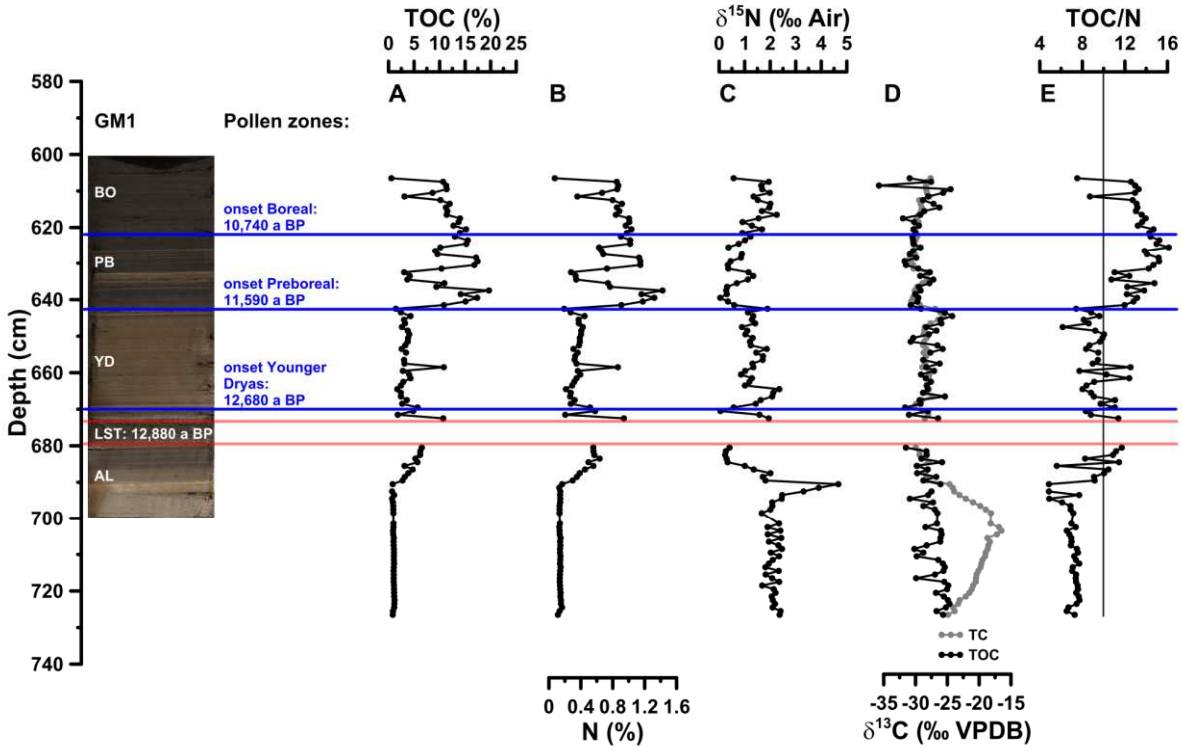

Fig. 3: (A) Depth profiles of (~~D~~A) ~~total and~~ total organic carbon (~~TC,~~ TOC), (~~E~~B) total nitrogen (~~T~~N), (~~F~~C) bulk stable nitrogen isotope composition (δ^{15}N), (~~G~~D) ~~TC and TOC~~ stable carbon isotope composition of total carbon (TC) and TOC ($\delta^{13}C_{TC}$, $\delta^{13}C_{TOC}$)~~,~~ and (~~H~~E) ~~C~~ carbon to nitrogen ratio ~~based on total organic carbon and total nitrogen~~ (TOC/~~T~~N). The vertical line in (~~H~~E) indicates a TOC/N ratio threshold of ~~12~~10 (Meyers, 2003). AL = Allerød, YD = Younger Dryas, PB = Preboreal~~,~~ and BO = Boreal.

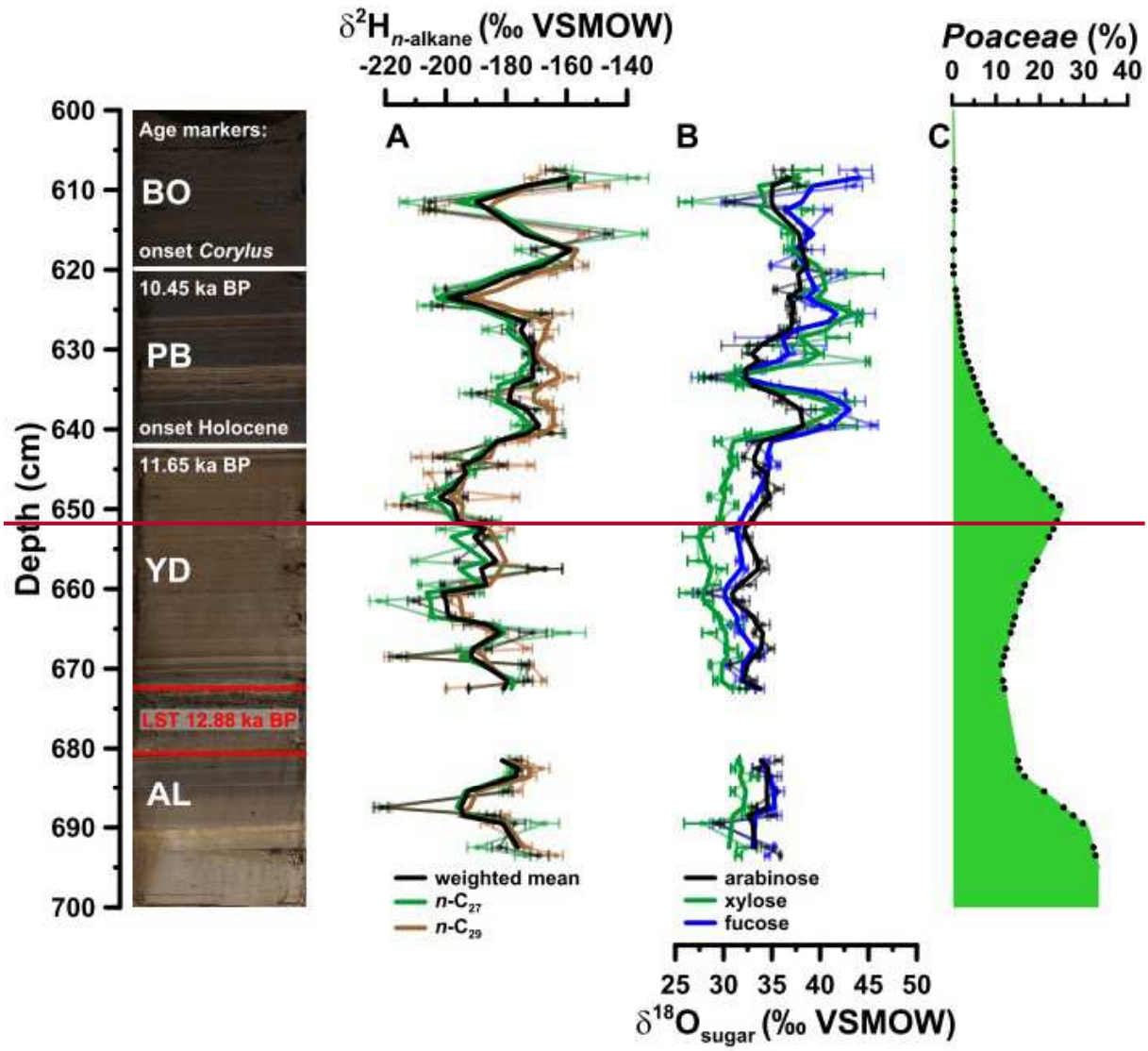
δ2Hn-alkane (‰ VSMOW)
-220 -200 -180 -160 -140
Poaceae (%)
0 10 20 30 40
A
B
C
Depth (cm)
600
610
620
630
640
650
660
670
680
690
700
Age markers:
BO
onset Corylus
10.45 ka BP
PB
onset Holocene
11.65 ka BP
YD
LST 12.88 ka BP
AL
weighted mean
n-C27
n-C29
arabinose
xylose
fucose
25 30 35 40 45 50
δ18Osugar (‰ VSMOW)

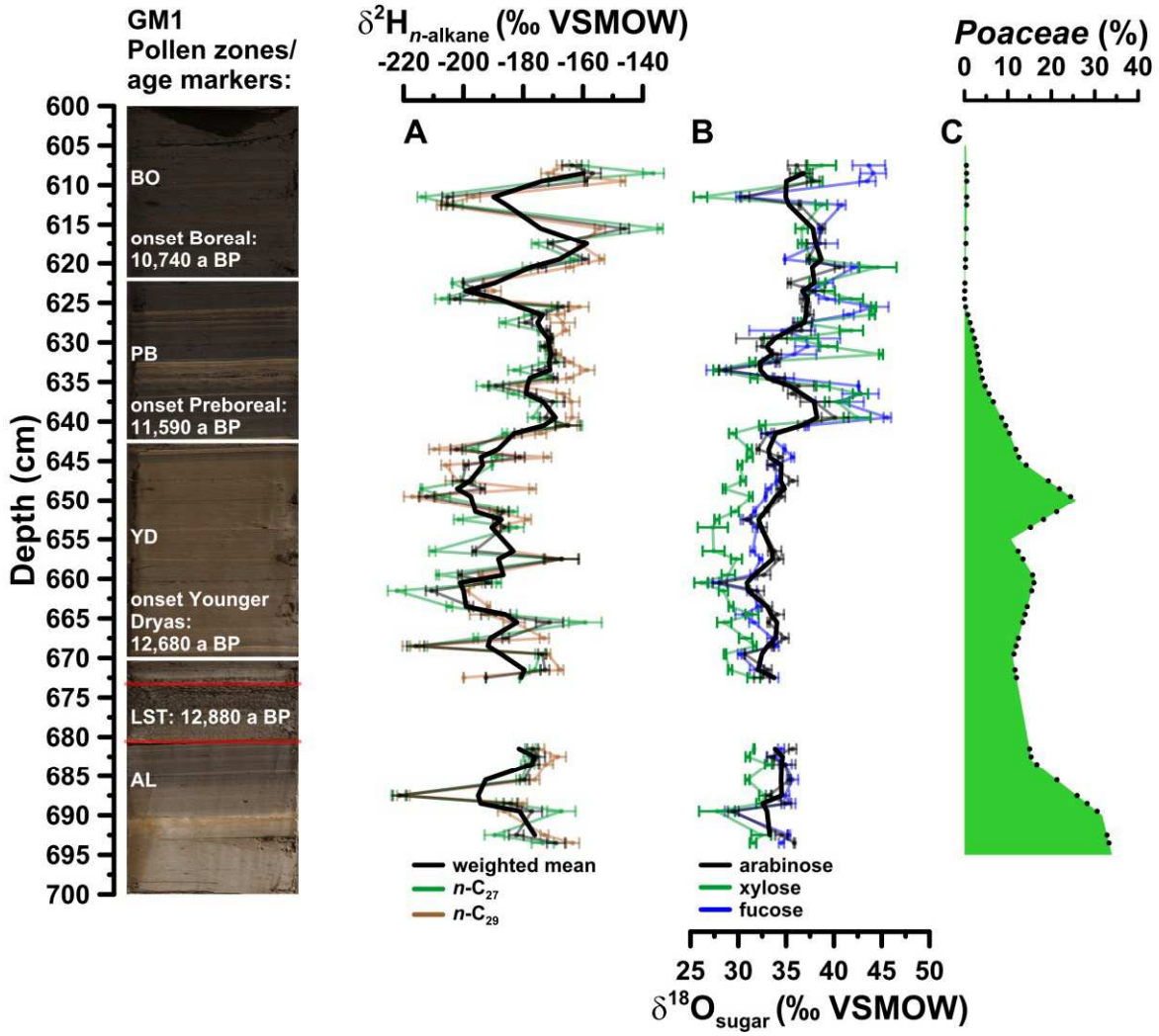

Fig. ~~3~~4: (A) Depth profiles of compound-specific stable hydrogen isotope composition of the individual alkanes *n*-C_{27} and *n*-C_{29} and the weighted mean ($\delta^2H_{n\text{-alkane}}$). (B) Compound-specific stable oxygen composition of the individual sugars arabinose, xylose and fucose ($\delta^{18}O_{sugar}$). ~~All plots are shown with e~~Error bars ~~representing~~ show analytical standard ~~measurement~~ errors, bold lines show ~~overlain by~~ three point ~~moving averages (bold lines)~~moving averages. (C) Depth profile of *Poaceae* pollen ~~(derived from unpublished pollen analysis by F. Sirocko)~~. Additionally, the resampled data points (black points) used for the grass correction procedures (Eq. 12 and 13) are displayed. In addition, the GM1 core picture with the used age markers is displayed. AL = Allerød, LST = Laacher See Tephra, YD = Younger Dryas, PB = Preboreal, and BO = Boreal.

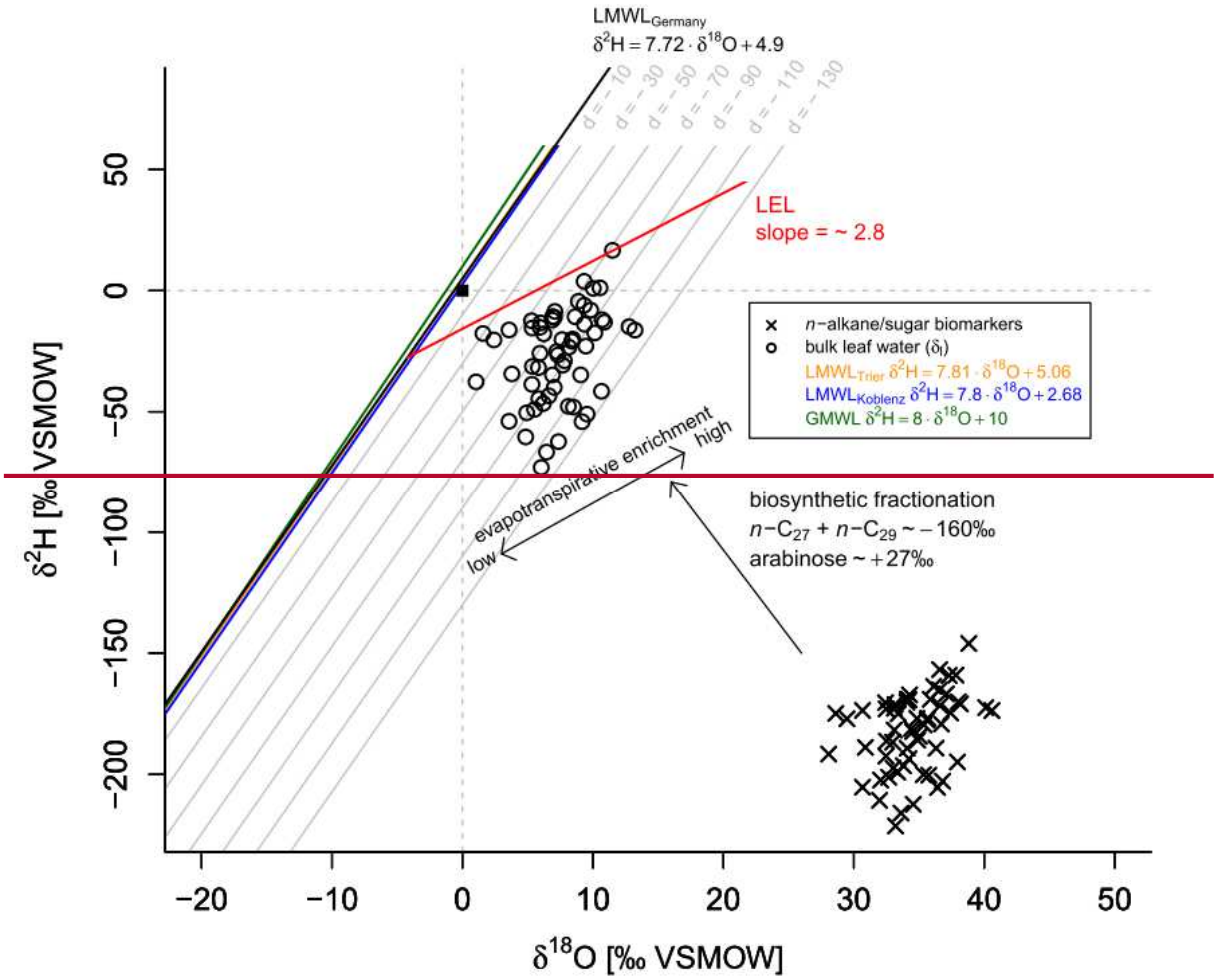
LMWL$_{Germany}$
$\delta^2H = 7.72 \cdot \delta^{18}O + 4.9$
d = −10
d = −30
d = −50
d = −70
d = −90
d = −110
d = −130
LEL
slope = ~ 2.8
n−alkane/sugar biomarkers
bulk leaf water (δ_l)
LMWL$_{Trier}$ $\delta^2H = 7.81 \cdot \delta^{18}O + 5.06$
LMWL$_{Koblenz}$ $\delta^2H = 7.8 \cdot \delta^{18}O + 2.68$
GMWL $\delta^2H = 8 \cdot \delta^{18}O + 10$
evapotranspirative enrichment
low
high
biosynthetic fractionation
$n-C_{27}$ + $n-C_{29}$ ~ −160‰
arabinose ~ +27‰
δ^2H [‰ VSMOW]
$\delta^{18}O$ [‰ VSMOW]
50
0
−50
−100
−150
−200
−20
−10
0
10
20
30
40
50

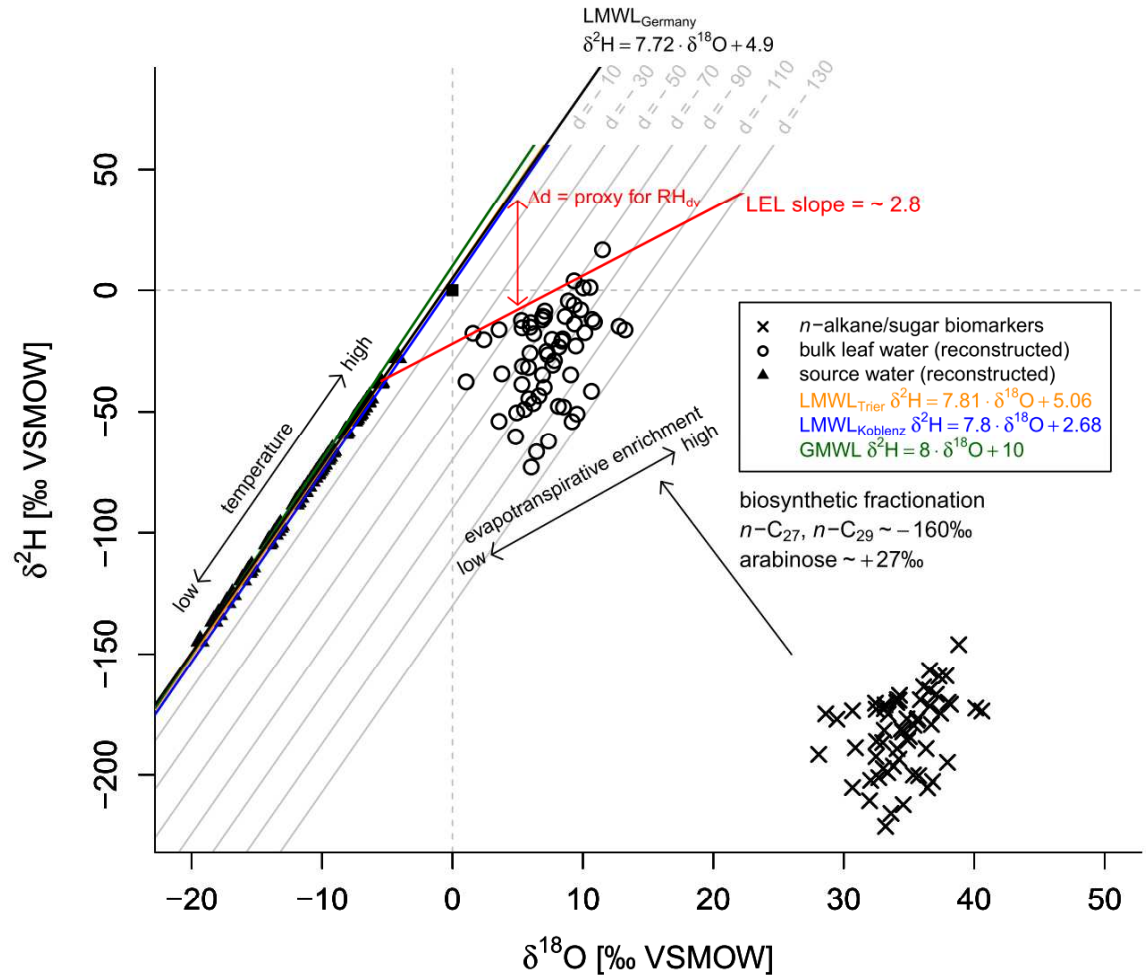

Fig. 45: (A) Conceptual framework of the ~~applied~~ coupled $\delta^2H_{n\text{-alkane}}$-$\delta^{18}O_{sugar}$ paleohygrometer approach displayed as $\delta^{18}O$-δ^2H diagram showing the measured *n*-alkanes (weighted mean of *n*-C_{27} and *n*-C_{29}) and sugar (arabinose) biomarkers (black crosses), the reconstructed leaf water (~~δ_l;~~ open circles), the global meteoric water line (GMWL, green line) and the local meteoric water lines of Germany ($LWML_{Germany}$, black line), Trier ($LWML_{Trier}$, yellow line) and Koblenz ($LWML_{Koblenz}$, blue line). The black arrows indicate natural processes of evapo~~r~~transpirative enrichment of leaf water along local evaporation lines (LEL), ~~and~~ biosynthetic fractionation during biomarker synthesis and the temperature effect on the source water isotope composition (~ precipitation). Grey lines indicate the parallel distance between the individual reconstructed evaporative site leaf water points and the $LMWL_{Germany}$, expressed as $d = \delta^2H - 7.72 \cdot \delta^{18}O$~~,~~ The difference between the d-excesses of the leaf water and source water ~~which~~ can serve as proxy for mean daytime vegetation period relative humidity (RH_{dv}; red double arrow).

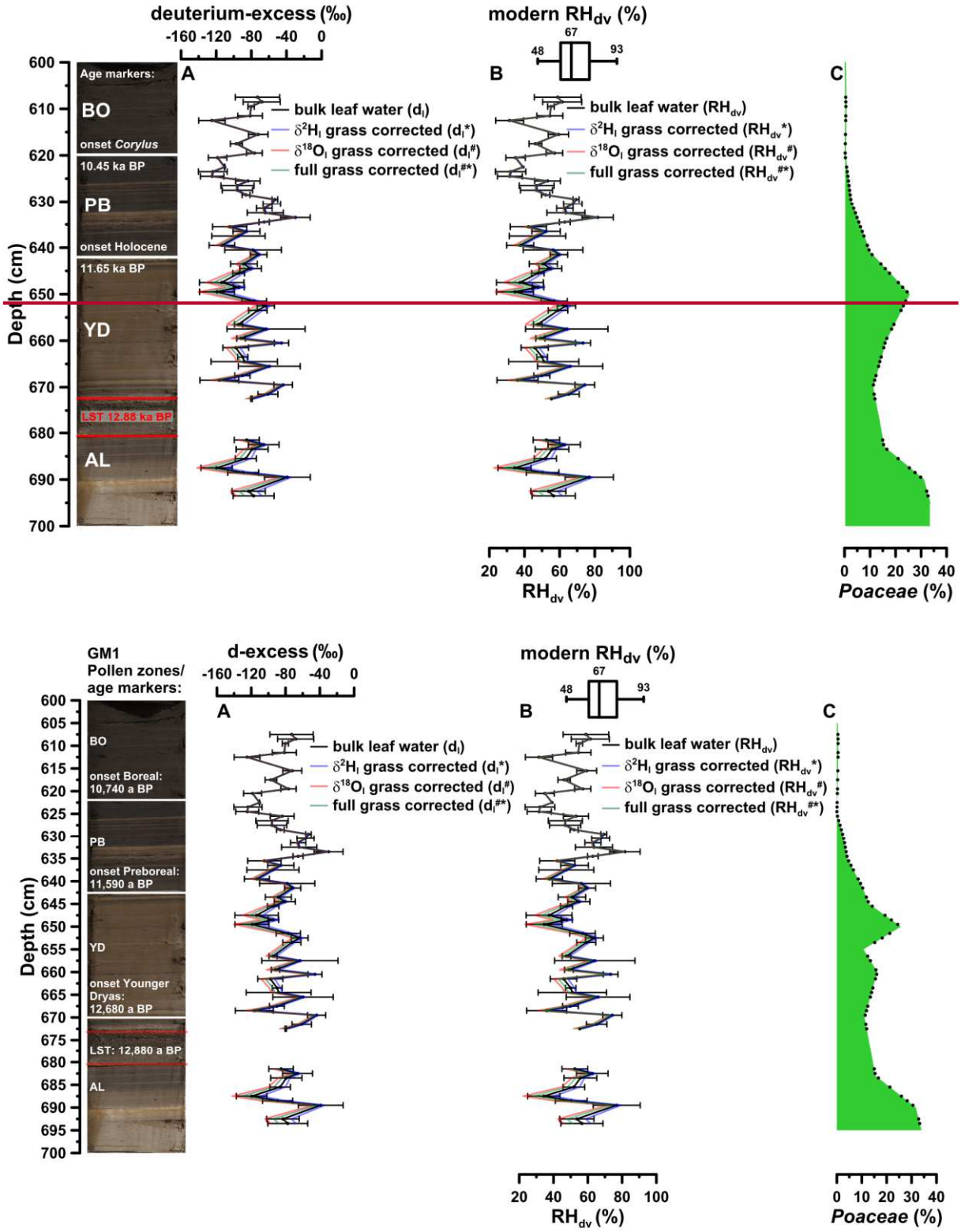

Fig. ~~5~~6: (A) ~~Reconstructed~~ deuterium-(d-)excess depth profiles ~~using~~ of reconstructed leaf water: ~~(~~d_l~~;~~ (black line) = no correction for grasses, ~~in comparison to solely *n*-alkane grass corrected~~ d_l* ~~values~~ (light blue line) = δ^2H corrected for grasses, ~~solely arabinose grass corrected~~ $d_l^{\#}$ ~~values~~ (light red line) = $\delta^{18}O$ corrected for grasses, ~~and full grass corrected~~ $d_l^{\#}$* ~~values~~ (light green line) = δ^2H and $\delta^{18}O$ corrected for grasses. The error bars of d_l values are calculated according to Eq. (7). (B) ~~The corresponding~~Reconstructed RH_{dv} records ~~to (A)~~.

Modern ~~relative air humidity~~RH variability during daytime and vegetation period (RH_{dv}) is displayed as boxplot derived from the adjacent meteorological station Nürburg-Barweiler, using monthly means from April to October between 6 a.m. and 7 p.m. (based on hourly data from 1995 to 2015; Deutscher Wetterdienst, 2016). The bold numbers within the boxplot represent~~s~~ the maximum, median, and minimum value~~s~~, respectively. (C) Depth profile of *Poaceae* pollen ~~(derived from unpublished pollen analysis by F. Sirocko)~~. Additionally, the resampled data points (black points) are displayed. The GM1 core picture with the used age markers are displayed on the left. AL = Allerød, LST = Laacher See Tephra, YD = Younger Dryas, PB = Preboreal, and BO = Boreal.

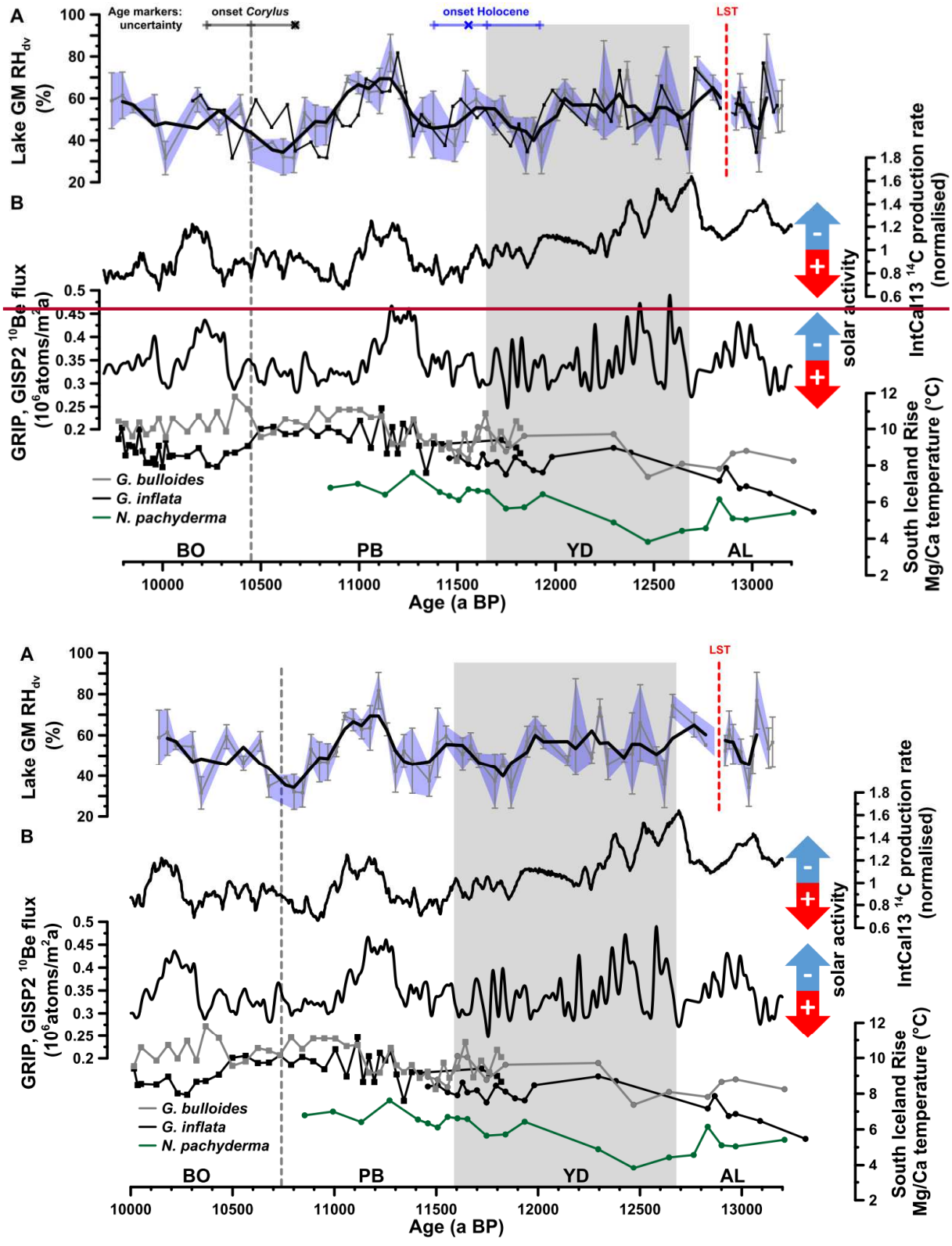

Fig. ~~6~~7: (A) Reconstructed ~~Lake~~ Gemündener Maar (GM) RH_{dv} ~~values~~record. The bold line shows the~~, overlain by a~~ three point moving average~~s (thick black line)~~. Error bars and the blue shaded area indicate analytical uncertainties ~~introduced by $^{2}H_{n\text{-alkane}}$/$^{18}O_{arabinose}$ measurements~~ calculated according to error propagation (Eq. 7). ~~In addition, the derived 68% uncertainty of the onset of *Corylus* pollen (black) and the Holocene (blue) are shown. The crosses within these~~

~~lines represents the adjusted ages according to the Monte-Carlo-Simulation based correlation procedure to the IntCal13 ^{14}C production rate. The GM RH_{dv} values are additionally shown on an optimized age-depth scale (thin black line with squares). Please note that the ^{14}C charcoal age is also covered by an error and was as well included in the adjustment procedure but not shown in this graph for clarity reasons.~~ (B) IntCal13 ^{14}C production rate, Greenland ice-core (GRIP, GISP2) ^{10}Be flux record (both from Muscheler et al., 2014) and South Iceland Rise planktic Mg/Ca derived water temperatures from RAPiD-12-1K (squares; ~~9,8~~10,000 to 11,800 a BP) and RAPiD-15-4P (circles; 10,900 to 13,~~100~~ 200 a BP). RAPiD-12-1K and RAPiD-15-4P *G. bulloides* and *G. inflat* data from Thornalley et al. (2009) and Thornalley et al. (2010), respectively. RAPiD-15-4P *N. pachyderma* data from Thornalley et al. (2011). Note that each record is plotted on its own timescale (planktonic Mg/Ca data see (Thornalley et al., 2009, 2010), ^{10}Be data on GICC05 (Rasmussen et al., 2006), ^{14}C data on IntCal13 calibration curve (Reimer et al., 2013) and RH_{dv} data on Lake GM age-depth model, see Fig. 2C). AL = Allerød, LST = Laacher See Tephra, YD = Younger Dryas, PB = Preboreal~~,~~ and BO = Boreal.

Table

~~Tab. 1: Scenarios (1-4) comprising the different reconstructed leaf water parameters based on the *n*-alkane/sugar biomarker, the respective equations used for this reconstruction, the resulting deuterium-excess of leaf water based on the reconstructed leaf water as input for Eq. (5) and the finally derived relative air humidity values during daytime and vegetation period (RH_{dv}) with this equation.~~

Tab. 1: Scenarios 1-4 used for reconstructing deuterium-(d-)excess of leaf water and corresponding RH_{dv} values in order to assess/estimate the effect of variable grass contributions on the reconstructed Gemündener Maar RH record (see also Fig. 6~~5~~).

scenario	leaf water reconstructed from *n*-alkane/sugar biomarkers	equations used for leaf water reconstruction	resulting d~~euterium~~-excess of leaf water as input for Eq. (5)	relative air humidity during daytime and vegetation period according Eq. (5)
1	$\delta^2H_l/\delta^{18}O_l$	(8) and (9)	d_l	RH_{dv}
2	$\delta^2H_l*/\delta^{18}O_l$	(8) and (9) + (11)	d_l*	$RH_{dv}*$
3	$\delta^2H_l/\delta^{18}O_l^{\#}$	(8) + (10) and (9)	$d_l^{\#}$	$RH_{dv}^{\#}$
4	$\delta^2H_l*/\delta^{18}O_l^{\#}$	(8) + (10) and (9) + (11)	$d_l*^{\#}$	$RH_{dv}*^{\#}$